RNI: DELENG/2005/15153
Publication: 23rd of every month
Posting: 27th/28th of every month at DPSO

No: DL(E)-01/5079/2023-25
Licensed to post without pre-payment U(E) 28/2023-25
Rs.150

ISSN 0973-2136

www.mycoordinates.org

Coordinates

Volume XXI, Issue 3, March 2025

THE MONTHLY MAGAZINE ON POSITIONING, NAVIGATION AND BEYOND

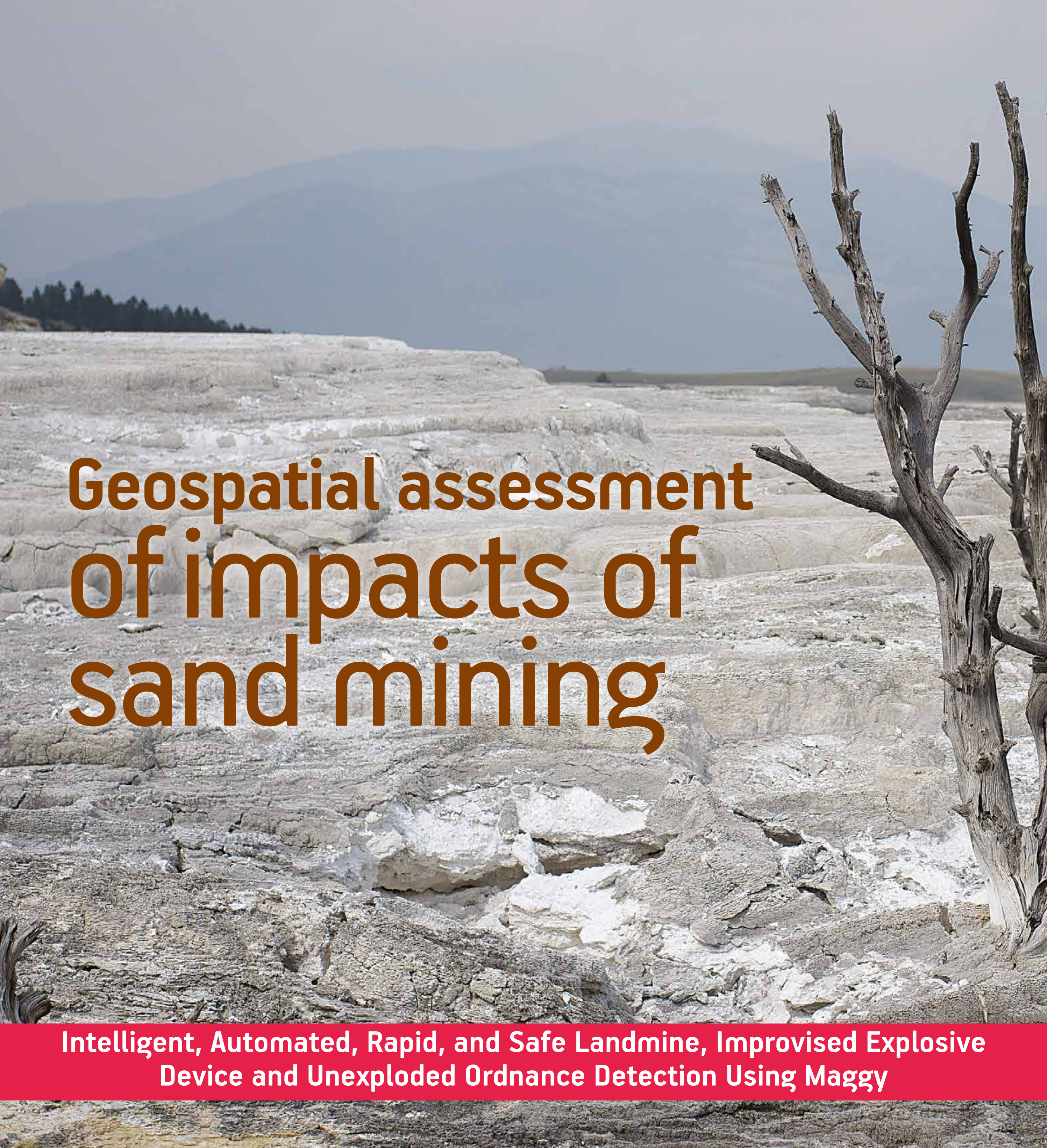

Geospatial assessment of impacts of sand mining

Intelligent, Automated, Rapid, and Safe Landmine, Improvised Explosive Device and Unexploded Ordnance Detection Using Maggy

In Coordinates

10 years before...

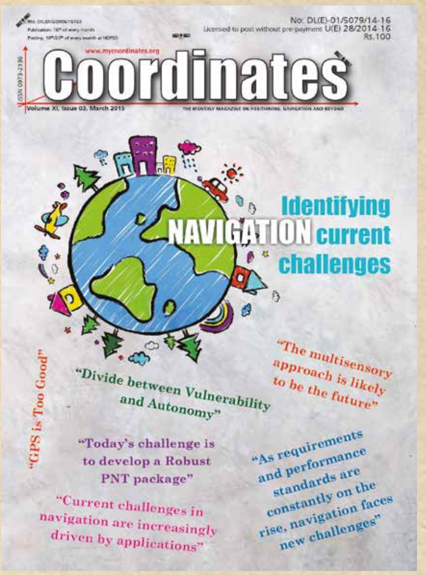

mycoordinates.org/vol-XI-issue-03-March-2015

Navigation – Current Challenges

The "Vulnerablists" declared that GNSS is fallible and dependent on weak signals, easily disrupted by noise and interference, some natural, some accidental and some- jamming and spoofing - malicious. You should not rely on GNSS but backit up with a different but complementary system. The clear leader here was eLoran which the UK General Lighthouse Authorities now had up and running, serving mariners (Gerard Offermans) and precise timing users (Charles Curry).

Professor David Last
Consultant Engineer and Expert Witness specialising in Radio Navigation and Communications Systems. Professor Emeritus at the University of Bangor, Wales and Past-President of the Royal Institute of Navigation

Multi constellation receivers make such spoofing more difficult – but not impossible. There is much work to be done.
Colin Beatty Fellow and Immediate Past President, of the Royal Institute of Navigation, Managing Director of CBi Ltd

Integrated systems are the likely future of navigation, with multi-system and multisensor generalizations decreasing vulnerability against system failure and attack.
Dorota A Grejner- Brzezinska, Professor and Chair, Department of Civil, Environmental and GeodeticEngineering, The Ohio State University

Challenges concerning timing are aimed to improve the precision of atomic clocks, enabling more accurate time and frequency synchronization over large distances.
Zbigniew Pietrzykowski Professor, Deputy Dean of Science, Faculty of Navigation, Maritime University of Szczecin, Poland

Current challenges in navigation, from a technology point of view, are more driven by the demand of high-sensitivity capability in combination with external sensors on one hand; and high position accuracy in combination with high reliability and integrity on the other.
Dr Guenter Heinrichs, Head of Customer Applications Business Development, IFEN GmbH, Germany

The solution to this complacency, to the problem that "GPS is too good," is a sensible agenda to protect, toughen and augment our Global Navigation Satellite Systems (GNSS).
Dana A. Goward, President, Resilient Navigation and Timing Foundation

A look into the future of positioning, navigation and timing

Dr Ing Marco Lisi
European Space Agency ESTEC, Noordwijk, The Netherlands

The advent of GNSS has made possible numerous advances in all area of our manufacturing and service economies and many critical infrastructures of our society would literally collapse in case of a total, worldwide GNSS failure. The world urgently needs an even stronger, more resilient and more versatile PNT infrastructure.

Managing inaccurate historical survey records in a future accurate digital world

Ian Harper
Director, Geodata Australia, Australia

When digital systems are being implemented there are two main transitions that can occur in representing boundaries. The manual to digital transition is the initial one, as any system needs to create a spatial representation of the cadastral boundaries in a digital format. All types of agreements, descriptive documents, maps and surveys need to be identified and represented for transaction requirements.

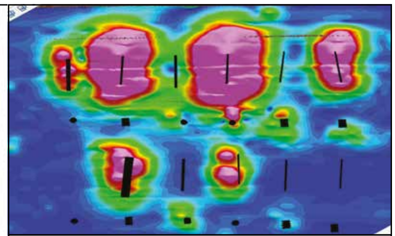

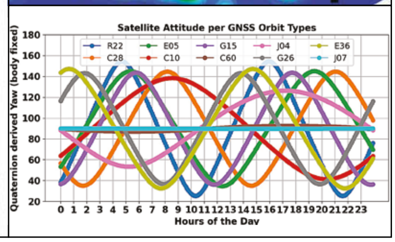

In this issue

Coordinates Volume 21, Issue 3, March 2025

Articles

Columns

This issue has been made possible by the support and good wishes of the following individuals and companies
Aadithya Sujit, Benjamin Jon Watkinson, Claire Tinker-Mill, Darren Ansell, John Michael Pinder, Haji Ali Haji, Kaya Kuru, David Jones, Narayan Dhital, Rahma Rashid Amour and Ridha Hamila; Riegl, SBG System, and many others.

Mailing Address
A 002, Mansara Apartments
C 9, Vasundhara Enclave
Delhi 110 096, India.
Phones +91 11 42153861, 98102 33422, 98107 24567

Email
[information] talktous@mycoordinates.org
[editorial] bal@mycoordinates.org
[advertising] sam@mycoordinates.org
[subscriptions] iwant@mycoordinates.org
Web www.mycoordinates.org

Coordinates is an initiative of CMPL that aims to broaden the scope of positioning, navigation and related technologies. CMPL does not neccesarily subscribe to the views expressed by the authors in this magazine and may not be held liable for any losses caused directly or indirectly due to the information provided herein.

Annual subscription (12 issues)
[India] Rs.1,800* [Overseas] US$100*
*Excluding postage and handling charges

Printed and published by Sanjay Malaviya on behalf of Coordinates Media Pvt Ltd
Published at A 002 Mansara Apartments, Vasundhara Enclave, Delhi 110096, India.
Printed at Thomson Press (India) Ltd, Mathura Road, Faridabad, India

Editor Bal Krishna
Owner Coordinates Media Pvt Ltd (CMPL)

This issue of Coordinates is of 36 pages, including cover.

DeGrokisation

The reliability of AI models is rooted in,

The "Garbage In, Garbage Out" principle,

Further worsened by algorithmic bias,

And the narratives set by the owners,

And controllers of these platforms.

Outsourcing the process of truth-seeking,

To machines that parrot patterns,

Not only hampers critical thinking,

But also runs the risk of drowning nuances in noises.

Over-reliance on AI may be,

Akin to walking into a trap

Garbage In, Gospel Out.

Bal Krishna, Editor
bal@mycoordinates.org

Intelligent, automated, rapid, and safe landmine, improvised explosive device and unexploded ordnance detection using Maggy

In this study, a small-scale customised drone – the so- called Maggy – was developed to simplify and automate the procedures of cleaning explosive devices. Readers may recall that we publsihed the first part of the paper in February issue. We present here the concluding part

Kaya Kuru
School of Engineering and Computing, University of Central Lancashire, Fylde Rd, Preston, Lancashire, PR12HE, UK

Aadithya Sujit
School of Engineering and Computing, University of Central Lancashire, Fylde Rd, Preston, Lancashire, PR12HE, UK

Darren Ansell
School of Engineering and Computing, University of Central Lancashire, Fylde Rd, Preston, Lancashire, PR12HE, UK

John Michael Pinder
School of Engineering and Computing, University of Central Lancashire, Fylde Rd, Preston, Lancashire, PR12HE, UK

David Jones
School of Engineering and Computing, University of Central Lancashire, Fylde Rd, Preston, Lancashire, PR12HE, UK

Benjamin Jon Watkinson
School of Engineering and Computing, University of Central Lancashire, Fylde Rd, Preston, Lancashire, PR12HE, UK

Ridha Hamila
Senior Member, IEEE, 2Department of Electrical Engineering, Qatar University, Doha, Qatar

Claire Tinker-Mill
School of Engineering and Computing, University of Central Lancashire, Fylde Rd, Preston, Lancashire, PR12HE, UK

Experimental Results

The functions of the prototype magnetometer-integrated autonomous drone – Maggy – were improved in the lab environments with numerous trial iterations and its viability in realising aforementioned targets was validated in the benchmark test fields with benchmark outputs as explicated in the following subsections. The use of the tablet application (Fig. 16) for the streamed data and old survey analysis is explained in [67] with a video.

A. Lab Tests With Maggy

In the lab environment, design of sensors and their integration with the drone components were extensively tested to find out i) the ideal component integration that avoids extreme magnetic interferences and ii) ideal configuration that ensures that subsequent sensor trials are reliable with repeatable and valid values under similar conditions. The acquired test data set was used to establish the classification and clustering algorithms with respect to the chosen MF threshold value (Fig. 16) as elaborated in Section III-B2.

The results obtained from the earlier trials in the lab environment with 1 m/s, 2 m/s, and 3 m/s flight speeds and 0.5, 1 m, and 2 m altitudes demonstrated

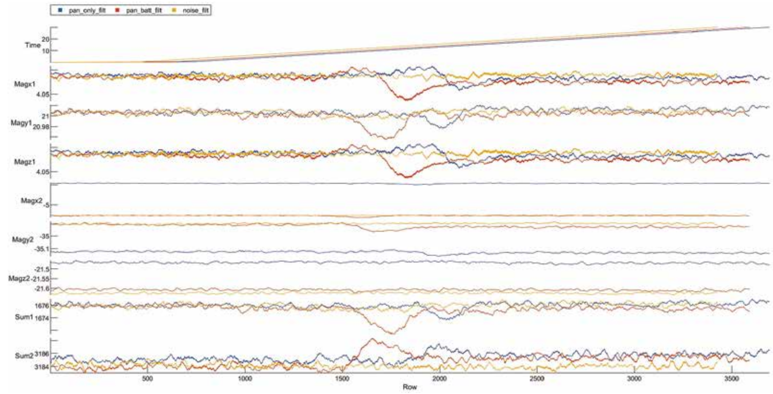

FIGURE 17. Change of MF values in the three axes with the two magnetometers when encountered a high MF. The total magnetic strength/intensity is shown at the bottom for two magnetometers.

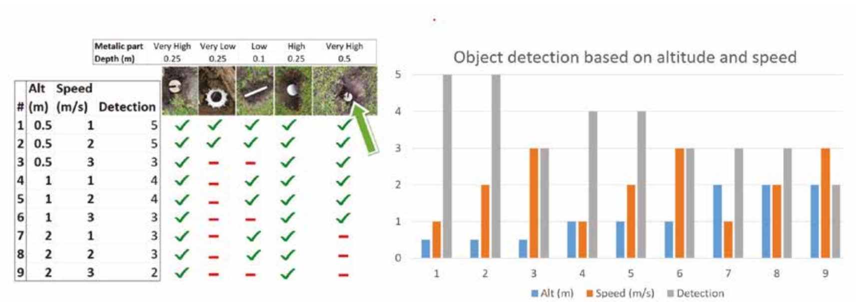

FIGURE 18. Nine test scenarios: The test results of Maggy for 5 different types of landmines with varying features. The green arrow shows the direction of Maggy during testing for each landmine separately. Maggy operates with high detection accuracy at low altitudes and speeds (i.e., 0.5 m, 1 m/s).

that 1 m/s flight speed and 0.5 m altitude outperformed other parameters, namely, 2 m/s, and 3 m/s flight speeds and 1 m, and 2 m altitudes. More specifically, the detection accuracy of MF decreases significantly, primarily, for the explosives with less metallic parts, as the flight/sensor

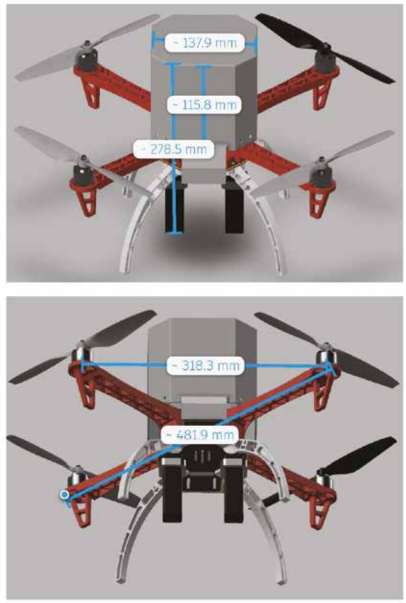

FIGURE 19. Shielded Maggy.

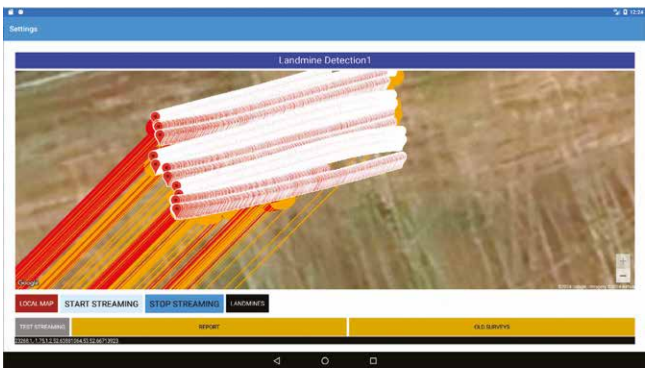

FIGURE 20. Autonomous use of Maggy in the UCLan landmine field. All data points.

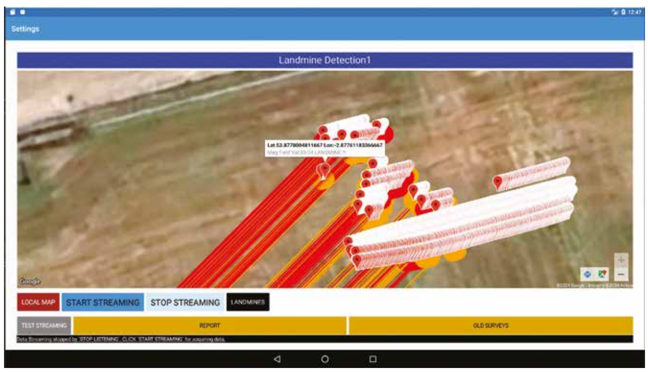

FIGURE 21. Landmine locations, until the current scanned point in the route, shown by user during data streaming while Maggy is still in operation.

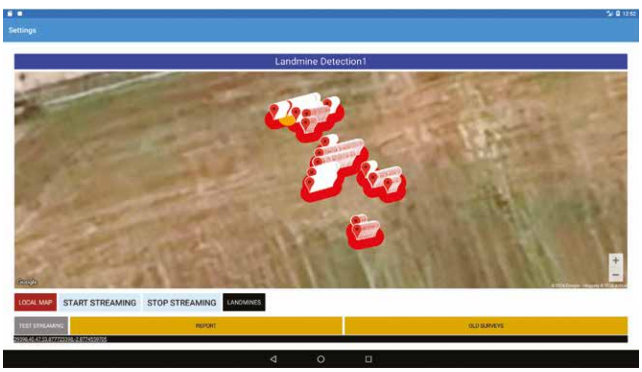

FIGURE 22. All landmine locations, with "very high" MF (red), shown by the user.

FIGURE 23. Landmine locations, with "very high" (red) and "high" (orange) MF, shown by the user.

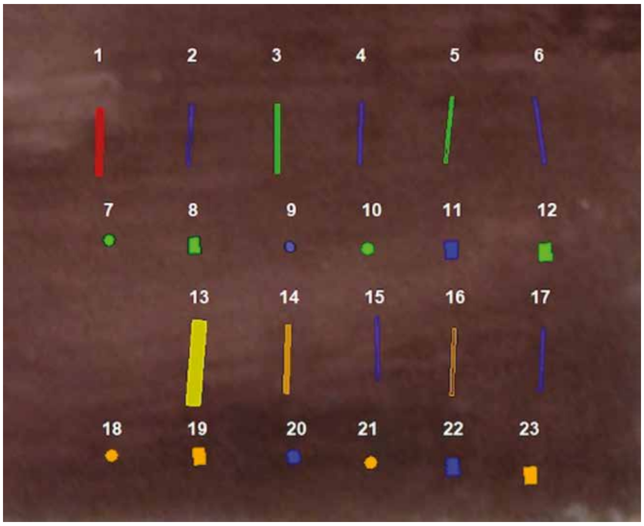

FIGURE 24. Latvia landmine/UXO/IDE field locations (Table 5).

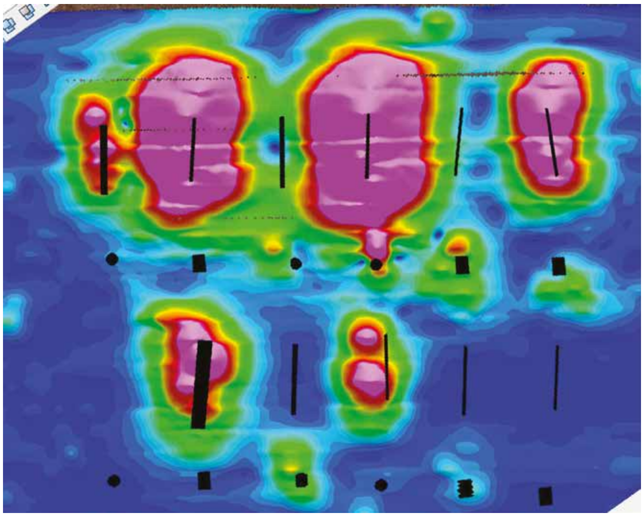

FIGURE 25. Geometric measurement of MF of the objects depicted in Fig 24) using the MagArrow Magnetometer[8].

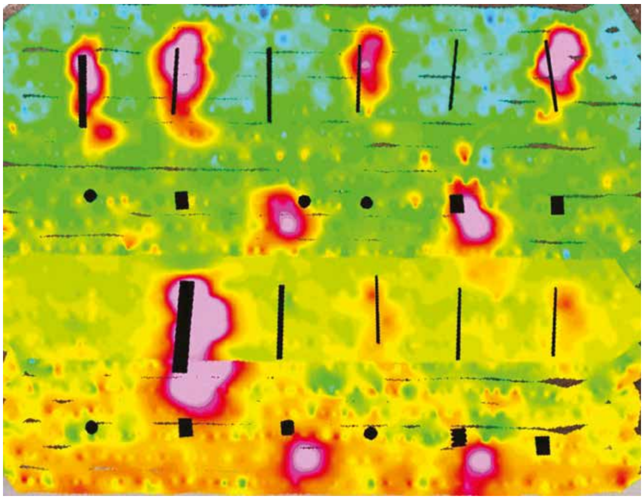

FIGURE 26. Geometric measurement of MF of the objects depicted in Fig 24) using the metal detector[9].

altitude increases and the flight speed increases. The MF values of various landmine/UXO/IDE were measured by Maggy and one of the acquired results is presented in Fig. 17. The change of MF values in the X, Y, and Z axes with the two magnetometers are demonstrated. The MF values of the targeted object can be distinctively noticed when encountered a high MF. The test results of 9 test scenarios for 5 different types of landmines with varying features are presented in Fig. 18. The noise level considerably rises with the speed increase. The increase in altitude hinders the ability to detect buried objects at deeper depths. The lesser the metallic parts the lesser the magnetic field. Operating at a height of less than 0.5 m (e.g. 0.25 m) not only puts operation safety at risk despite the terrain following capability of Maggy, but the echoed acoustics from the ground also significantly increase noise levels, making the detection impossible. Maggy operates with high detection accuracy at low altitudes and speeds (i.e., 0.5 m, 1 m/s). Maggy was tested in real benchmark test fields as explained in Section IV-B after it passed its tests in the lab environment. To summarise, the test results in the lab environment were instrumented to determine the ideal parameters for Maggy considering its design and configuration.

B. Real Field Tests With Maggy

Maggy was covered with a shield as shown in Fig. 19 to protect the electronics from bad weather conditions, especially, from rain. In this way, Maggy can function under rainy conditions. It is noteworthy to emphasise that Maggy cannot resist heavy windy conditions due to its lightweight design. Maggy operated with 1 m/s flight speed and 0.5 m altitude. The ability to fly under 1 m altitude and very low speed increases the magnetometer sensor performance significantly as explained in Section IV-A. Maggy was tested in the UCLan landmine field and the Latvia test field.[7] The results of these tests are explained in the following subsections.

1) Real Field Tests with Maggy at the Uclan Landmine Field

The landmines in the UCLAn landmine field (Fig. 6) were buried between 15 cm to 50 cm depth as shown in Fig. 9. Several off-the-shelf UAV-mounted sensor modalities such as GPR and magnetometer (Fig. 5) were already tested by the UCLan ASR team successfully. In those tests, the MF map of the UCLan landmine field was constructed with detailed information as shown in Fig. 7 and the disclosed landmine field spots are shown in Fig. 8. The UAS, flying with an altitude of 1 m at a 1 m/s flight speed (Fig. 6), was able to detect 21 landmine spots out of 25 successfully with an accuracy rate of 0.84. The large size of the drone, causing high noises with interferences, i.e., the echoed acoustics from the ground at an altitude lower than 1 m, didn't let us fly at lower altitudes. Consequently, 4 landmines weren't detected where 2 of them, composed of large metallic parts, were at the depths of 0.5 m and 0.25 m and the other 2 of them, composed of little metallic parts, were at the depths of 0.5 m and 0.25 m. Maggy was deployed in the same landmine field in an autonomous mode with the previously tracked waypoints to conclude if the developed approaches considering all the components of Maggy and their integration with one another were functioning as desired. The MF formation of the landmines with metallic objects is demonstrated through real-time data streaming in the IEEE DataPort [67] with a video using the earlier version of the application. All scanned points are displayed in Fig. 20. The "very high MF" locations, highlighted by red colour, are disclosed in Fig. 22 and "high MF" locations, highlighted by orange colour, are shown in Fig. 23 together with the "very high MF" locations. Maggy was found to be performing satisfactorily in revealing the pre-mapped MF locations (Fig. 8). Maggy was successful in finding 24 landmine spots out of 25. One landmine at a depth of 0.5 m with little metallic part couldn't be detected by Maggy. It is noteworthy to emphasise that "very high MF" locations (red) are surrounded by "high MF" (orange), which indicates that Maggy can show the hot/red MF spots inside orange circles when the field is scanned densely. Fig. 21 shows that the user can disclose the previous hot spots while Maggy, with multi-processing ability, is in operation. Maggy accomplished its operational objectives in these field tests in finding landmines with metallic parts, having an accuracy rate of 0,96. This field test demonstrated that the development of lightweight drones like Maggy, with reduced interferences/noise enabling low-altitude flights, improves the detection of landmines/IDE/UXO significantly.

2) Real Field Tests With Maggy at the Latvia Field

The size of the Latvia test field is 450×70 meters with permanently installed objects as elaborated in Table 5 and as illustrated in Fig. 24. The MF formation of the field was already obtained as presented in Figs. 25 and 26 using two different sensor modalities, namely, the MagArrow magnetometer and metal detector. Maggy can rapidly scan a large terrain, providing near real-time survey data. However, Maggy flew a few straight lines over known targets as displayed at the top of Figs. 27 and 28 due to the battery limit during our flight from the UK to Latvia. The battery does not last very long. Each full battery can function for up to 4 min 30 sec at low-speed flying, which restricts the scanning of larger areas, especially, at the ideal speed of 1 m/s. This testing provided us with data on the system's sensitivity to detect objects with various quantities of metal content, at various depths, in different soil/surface materials. Maggy was successful in detecting objects in this field as presented in the middle of Figs. 27 and 28. The histograms of MF values along with those straight lines are shown at the bottom of Figs. 27 and 28. The MF locations can be distinctively noticed in those graphs. Maggy completed its operations over 9 objects with metallic parts (Figs. 25 and 26) and it was successfully in spotting the pre-generated high-field areas with a success rate of 1.0. This field test demonstrated that Maggy could detect objects placed at deeper depths such as 1 m and further if these objects have larger metallic parts, enabling large MF. The real-field tests help us understand the abilities as well as the shortcomings of Maggy in operations to find out the improvement points (Table 6) in its design and functionalities, which is discussed and elaborated in Sections V, VI, VII and VIII in different perspectives.

Discussion

Landmines pose a significant threat to civilian populations and humanitarian efforts worldwide in addition to its economic loss as pointed out earlier. Heavily mined low-income countries often cannot afford high-tech landmine/UXO/IDE demining equipment to expedite the clearing activities. Despite the intensive effort spent in finding an effective and efficient approach to demining, a safe semi/fully autonomous method is yet to be realised in finding landmines rapidly and safely in a cost-effective manner. Since the end of the eighties, the start of the first humanitarian mine clearance operations in Afghanistan, the metal detector is still the only trusted sensor used in humanitarian demining [7]. Any technique still needs to be confirmed with a detector to ensure the location of landmines. Detecting and safely removing landmines is crucial for the safety and well-being of affected communities. Therefore, deploying robots for these types of work is vitally important due to their very high potential risks. Autonomous robotic applications are replacing the human force, in particular, for dangerous and labour-intensive tasks in many areas.

Cost-effective UAVs equipped with advanced sensors and AI offer a promising solution for efficient and accurate landmine/UXO/IDE detection. This research aims to develop an integrated drone system capable of detecting landmines/IDE/UXO using magnetometers, and AI-based classification and clustering algorithms ([68]). The evaluation of the developed aerial platform was carried out by processing the experimental data gathered in controlled conditions at the lab and real benchmark test sites. Successful outcomes of the tests in this research show that the platform can empower the humanitarian clearing teams towards the aforementioned challenges, particularly, the threat of explosive devices. Maggy can scan a large area quickly and provide a real-time map of MF generated by on-ground and underground metallic objects. Its compact size enables numerous applications in many demining use cases by providing real-time surveying data. The benefits are a risk reduction to the demining clearing personnel, and/or their vehicles, an increase in safety and an increase in assurance of information. Drone-mounted magnetometers are suggested to be separated from UAS to avoid magnetic interference ([64], [65], [66]) as shown in Fig. 2. But, this increases the motion noise in addition to the wind noise. Other magnetometer systems tend to be physically large, limiting their application to wider open areas with forgiving terrain, expensive, and do not give real-time results which is not desirable to promote freedom of movement. This research shows how the detection and removal of

TABLE 5. Properties of buried objects depicted in Fig 24. Di: Diameter (mm); L: Length (m); D:Depth (m).

#	Target	Di	L	D
1	Stainless steel pipe	110	6.0	0.4 - 1.0
2	Steel pipe 4.0mm wall	500	6.0	1.0 - 2.0
3	PVC pipe EMPTY	110	6.0	0.4 - 1.0
4	Steel pipe 3.0mm wall	314	6.0	1.0 - 2.0
5	PVC pipe EMPTY	160	6.0	0.5 - 1.5
6	Steel pipe 2.5mm wall	200	6.0	0.5 - 1.5
7	Plastic barrel 50L vertical (empty)	400	0.57	0.5
8	Plastic barrel 50L horizontal (empty)	400	0.57	0.5
9	Steel barrel 200 L, vertical	610	0.88	1.0
10	Plastic barrel 100L vertical (empty)	420	0.70	1.0
11	Steel barrel 200 L, horizontal	610	0.88	1.0
12	Plastic barrel 100L horizontal (empty)	420	0.70	1.0
13	Reinforced concrete pipe	1000	8.0	1.0 - 2.0
14	PVC pipe (water filled)	110	6.0	0.4 - 1.0
15	Steel pipe 3.0mm wall	60	6.0	0.5 - 1.5
16	PVC pipe (water filled)	160	6.0	0.5 - 1.5
17	Steel pipe 1.5mm wall	110	6.0	0.5 - 1.5
18	Plastic barrel 50L vertical (water filled)	400	0.57	0.5
19	Plastic barrel 50L horizontal (water filled)	400	0.57	0.5
20	Steel barrel 200 L, diagonal	610	0.88	1.0
21	Plastic barrel 100L vertical (water filled)	420	0.70	1.0
22	Steel barrel 200 L, flattened (crashed)	610	0.88	1.0
23	Plastic barrel 100L horizontal (water filled)	420	0.70	1.0

metallic explosives in humanitarian mine clearance operations can be significantly accelerated by UAVs fitted with magnetometers. The ability to fly under 1 m altitude using an altimeter and at a very low speed (i.e. 1 m/s) increases the magnetometer sensor performance significantly compared to the other flight parameters based on the results obtained from the earlier trials in the lab environment (Section IV-A). The main goal of this research is to host the sensor system on small lightweight robust aerial platforms that can be carried in a backpack and rapidly deployed by humanitarian demining teams. Our idea was born from many years of work, researching the detection of buried landmines using drone-mounted sensors. The design of Maggy has been heavily influenced by real conditions on the ground and after consultation with mine clearance organisations. This research demonstrates that MF generated by landmine/UXO/IDE substantially depend on the depth of objects and the magnitude of the metallic parts. In other words, signatures of buried explosives are site-dependent. Therefore, the developed classification and clustering techniques in this research use field-dependent data sets, without needing a priori training set. All the datasets related to this work will be uploaded to the IEEE DataPort [67] for the researchers who would like to perform similar studies, which will lead to new

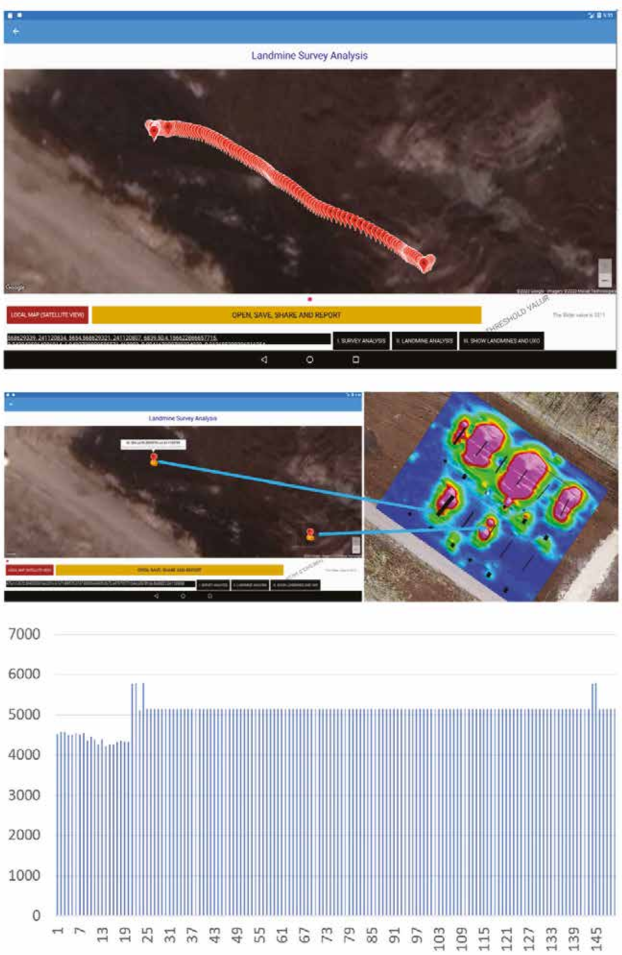

FIGURE 27. Latvia field test -III-. Top: all data points; middle: high MF; bottom: MF graph for all data points in the route depicted at the top.

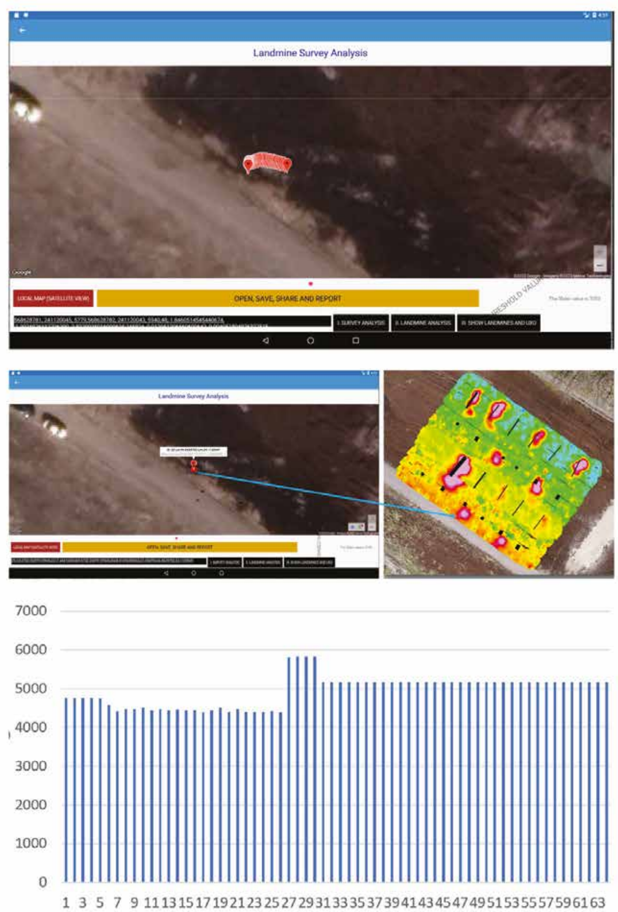

FIGURE 28. Latvia field test -I-. Top: all data points; middle: high MF; bottom: MF graph for all data points in the route depicted at the top. MF is clearly very high at the above location (middle) as shown in the histogram points between 25 and 31.

directions in this specific field. While not all ordinances will have a magnetic signature, many will and on balance risk can be reduced by deploying this system. Maggy's capabilities as well as its features are evaluated in Table 6 with multiple criteria put forth by mine clearance organisations and the current literature research. The study presents a compelling exploration into the use of drones for detecting landmines, IEDs, and UXOs. The integration of advanced sensor technologies, particularly magnetometers, shows the potential of UAVs in humanitarian demining operations, offering a rapid and efficient means of surveying large areas that are often difficult to access. One of the most imperative aspects of this research is the innovative application of UAVs in a domain that is critical for safety and humanitarian efforts. The capability of Maggy to provide near real-time data has the potential to enhance the efficacy of mine clearance operations, potentially saving lives and resources. This research effectively highlights the advantages of using drones over traditional ground-based methods, particularly in terms of speed and safety. Maggy is innovative in the following ways:

- It has been designed to be compact and lightweight.
- It can provide near real-time scanned streaming data to the user, which is displayed on a small tablet/smartphone device.
- It is low-cost compared to commercially available magnetometer systems.
- The application can filter streaming data quickly, providing the classification of MF spots as very high, high, moderate, low and very low.
- Multiple numbers of similar platforms can be deployed as a swarm to expedite the clearing process. The developed application can stream data from multiple platforms simultaneously.

TABLE 6. Evaluation of Maggy.

#	CRITERIA	✓/-	NOTES
1	Detection of all explosive types	-	only explosive objects with ferrous metals can be detected by Maggy.
2	Determination of the type and composition of metallic objects	-	only MF location of metallic objects can be detected.
3	Small and light weight	✓	Fig. 19, payload < 1 kg.
4	Manoeuvrable	✓	rotary, vertical take-off and landing.
5	Terrain following mode	✓	Maggy uses a radar altimeter.
6	Autonomous/automated mode	✓	Maggy uses UgCS system – drone flight planning software.
7	Low energy consumption	✓	Fig. 19, payload < 1 kg, most of the processing and computing is performed by the tablet application.
8	Good flight time, long battery life	-	Maggy can fly 4.5 minutes per battery
9	Robust	✓	Maggy was designed to perform robustly (Figs. 11, 12, 13, 14). The GPS component will be replaced with a robust one.
10	Accurate/reliable	✓	Maggy is tested in the benchmark test fields with the benchmark outputs.
11	Air-to-ground data streaming	✓	Maggy provides near real-time scanned streaming data to the user while in operation.
12	Real-time data processing	✓	Maggy provides real-time scanned streaming data to the user, which is displayed on a small tablet/smartphone device.
13	Easy to use/off the shelf	✓	Maggy is a compact tool.
14	User friendly	✓	30 minutes of training is sufficient to use Maggy effectively.
15	Resource friendly	✓	not resource-hungry processing. Ability to run ordinary computing device.
16	Ability to analyse old surveys	✓	AI-based tablet/smartphone application provides users with multiple decision-making abilities.
17	Classification and clustering abilities	✓	AI-based tablet/smartphone application provides users with multiple decision-making abilities.
18	Ability to fly under 1 meter	✓	to increase the efficacy of sensors.
19	Small footprint	✓	Fig. 19, payload < 1 kg.
20	Accessible, low-cost, affordability	✓	Maggy is low-cost compared to commercially available magnetometer systems.

Conclusion

The cost of clearance is estimated to be USD 300-1000 per mine using conventional techniques and 1 person dies for every 5000 mines removed [69]. Mine clearing needs are in high demand all around the world. This study mainly aims to build new fully automated landmine/UXO/IDE detection systems in a time-and-cost-efficient manner. Capable of vertical take-off and landing and flying at very low altitudes with low speed makes rotary drones easy to use and efficient in humanitarian clearing operations, if equipped with effective sensor technologies and AI with proper configurations. The near real-time data provided by a UAV-integrated magnetometer system can greatly improve mine clearance operations. In this direction, the methods created in this study address the drawbacks of ground-based operations, such as high operator risk and inefficiency, and provide a quicker, safer, and more economical substitute for conventional landmine/UXO/IDE detection techniques. The developed platform in this work, the so-called Maggy, is a small, lightweight drone that can be rapidly deployed by a demining team to scan a large area for any magnetic anomalies caused by the presence of metal in landmine/UXO/IDE. It helps accelerate the speed of clearing operations across large and tough terrains or other hazardous land areas, reducing risk, increasing assurance, and improving safety for the humanitarian team. More specifically, as evaluated in Table 6, the compact, lightweight, real-time magnetometer aerial surveying system – Maggy – can scan for the presence of ferrous metal, and real-time detection information is displayed on a tablet/ smartphone device (Fig. 16). The tablet/smartphone application ([67]) overlays detection information on a satellite map image of the survey site. Highly risky terrains can be surveyed by cost-effective Maggy to turn the area into low-risky areas using safer and faster scanning approaches than conventional methods. The risk to human operators can be reduced significantly with Maggy. This research provides the related research community and industry with fundamental design and implementation parameters (e.g. flight speed, flight altitude) in building and using magnetometer-integrated UAS.

Limitations

The features of Maggy are evaluated in Table 6 with its shortcomings. Maggy uses only magnetometer sensors which detect MF created by metallic objects. Therefore, landmines/IDE/UXO with no or fewer metallic objects may not be detected. Maggy cannot operate long due to its short battery life, which necessitates the use of multiple batteries for consecutive operations. The type and composition signature of metallic objects cannot be determined by Maggy. The use of Maggy is suggested in detecting explosives which consist of large metallic objects and in detecting metallic landmines. Additionally, Maggy cannot function properly under heavy windy conditions due to its lightweight feature.

Future Research Ideas

The battery life and operating time of Maggy in the field will be enhanced. We aim to develop another UAS, that is fully integrated with Maggy, to spray/paint red/high MF spots to direct clearance teams appropriately in reducing risks while Maggy is in operation. A quadrotor drone equipped with magnetometers [70] demonstrated the necessity of combining magnetometer data with other geophysical techniques to improve detection accuracy considering all types of explosives. In this direction, sensor data fusion is successful and a way to decrease the number of false alarms for detection [1], [71]. Multiple sensors can be employed simultaneously to fuse the acquired data instances at a time for better decision-making (Fig. 7). We would like to incorporate other sensor modalities such as GPR and vision-based remote sensing sensor modalities (i.e. IR, LWIR camera, and multispectral camera) into Maggy as the size and weight of these modalities decrease. UCLan and Qatar University are collaborating on a funded project to build bespoke drone systems with the major sensor modalities.

The results of this work confirm the viability of our aerial-based system. Therefore, Maggy can be deployed in real minefields in mine-plagued countries such as Afghanistan, Cambodia and Croatia to support the removal of the landmines safely. Maggy will be tested in Cambodia in larger mine-affected areas in cooperation with the Cambodian Army to quantify the observed results in more difficult scenarios. Current results show promising directions for future research ideas. Similar studies continue to be an area of active interest involving other industries. The techniques and approaches developed in this research can be exploited by various industries for a wide spectrum of application areas such as aerospace, defence, and archaeology as well, in particular, for archaeological surveys, infrastructure inspection, the detection of buried metallic objects, forensic investigations, and security applications. More explicitly, Maggy can help locate artefacts, buried structures, and archaeological sites without the need for excavation. Additionally, real-time automatic mine detection on battlefields can be carried out by Maggy.

In conclusion, while the Maggy presents a promising advancement in UAV technology for humanitarian applications, for future work, it would be beneficial to explore the implementation of a UAV swarm strategy. Utilizing multiple drones could enhance coverage and efficiency, allowing for simultaneous scanning of larger areas and potentially compensating for individual UAV limitations. Furthermore, optimizing battery performance through improved capacity or better battery management systems as well as low-power sensors ([72]) could significantly extend mission durations and enhance operational effectiveness.

Acknowledgment

The funding agreement ensured the authors' independence in designing the study, interpreting the data, writing, and publishing the report. The views expressed are those of they and not necessarily those of the funder. They would like to express their deepest gratitude to the staff working at the test sites. They would like to thank the anonymous reviewers for their constructive input and comments.

Footnotes

[1] https://www.de-mine.com/projects-1

[2] https://www.de-mine.com/projects-1

[3] https://sensysmagnetometer.com/products/magdrone-r4-magnetometer-for-drone/

[4] https://www.smithsonianmag.com/innovation/a-ukrainian-teenager-invents-a-drone-that-can-detect-land-mines-180980826/

[5] https://www.uclan.ac.uk/business/support-for-smes/lancashire-innovation-drone-zone

[6] https://qrdi.org.qa/en-us/Scientific-Research/Academic-Research-Grant-ARG

[7] https://www.sphengineering.com/integrated-systems/test-range-for-geophysical-sensors

[8] https://www.geomatrix.co.uk/land-products/magnetic/magarrow/

[9] https://geonics.com/html/em61-mk2.html

References

[1] K. Kuru, D. Ansell, B. J. Watkinson, D. Jones, A. Sujit, J. M. Pinder, and C.L. Tinker-Mill, "Intelligent automated, rapid and safe landmine and unexploded ordnance (UXO) detection using multiple sensor modalities mounted on autonomous drones," *IEEE Trans. Instrum. Meas.*, 2024.

[2] M. Ihab, "Hyperspectral imaging for landmine detection," M.S. thesis, Politecnico Di Torino, Turin, Italy, 2017.

[3] H. Aoyama, K. Ishikawa, J. Seki, M. Okamura, S. Ishimura, and Y. Satsumi, "Development of mine detection robot system," *Int. J. Adv. Robot. Syst.*, vol. 4, no. 2, p. 25, 2007, doi: 10.5772/5693.

[4] S. B. I. Badia, U. Bernardet, A. Guanella, P. Pyk, and P. F. Verschure, "A biologically based chemo-sensing UAV for humanitarian demining," *Int. J. Adv. Robot. Syst.*, vol. 4, no. 2, p. 21, 2007, doi: 10.5772/5697.

[5] *Landmine Monitor 2015*, Int. Campaign Ban Landmines, Cluster Munition Coalition, OT, Canada, 2015.

[6] I. Makki, R. Younes, C. Francis, T. Bianchi, and M. Zucchetti, "A survey of landmine detection using hyperspectral imaging," *ISPRS J. Photogramm. Remote Sens.*, vol. 124, pp. 40–53, Feb. 2017. [Online]. Available: http://www.sciencedirect.com/science/article/pii/S0924271616306451

[7] D. Guelle, M. Gaal, M. Bertovic, C. Mueller, M. Scharmach, and M. Pavlovic, "South-East Europe interim report field trial Croatia: Itep-project systematic test and evaluation of metal detectors—STEMD," Federal Inst. Mater. Res. Test., Berlin, Germany, Rep. JRC32613, 2007.

[8] C. Castiblanco, J. Rodriguez, I. Mondragon, C. Parra, and J. Colorado, "Air drones for explosive landmines detection," in *Proc. 1st Iberian Robot. Conf.*, vol. 253, Jan. 2014, pp. 107–114.

[9] X. Zhang, J. Bolton, and P. Gader, "A new learning method for continuous hidden Markov models for subsurface landmine detection in ground penetrating radar," *IEEE J. Sel. Topics Appl. Earth Observ. Remote Sens.*, vol. 7, no. 3, pp. 813–819, Mar. 2014.

[10] C. P. Gooneratne, S. C. Mukhopahyay, and G. S. Gupta, "A review of sensing technologies for landmine detection: Unmanned vehicle based approach," in *Proc. 2nd Int. Conf. Auton. Robots Agents, Dec.* 2004, pp. 401–407.

[11] P. Gao and L. M. Collins, "A two-dimensional generalized likelihood ratio test for land mine and small unexploded ordnance detection," *Signal Process.*, vol. 80, no. 8, pp. 1669–1686, Aug. 2000. [Online]. Available: http://www.sciencedirect.com/science/article/pii/S0165168400001006

[12] W. Rafique, D. Zheng, J. Barras, S. Joglekar, and P. Kosmas, "Predictive analysis of landmine risk," *IEEE Access*, vol. 7, pp. 107259–107269, 2019.

[13] J. Colorado, I. Mondragon, J. Rodriguez, and C. Castiblanco, "Geo-mapping and visual stitching to support landmine detection using a low-cost UAV," *Int. J. Adv. Robot. Syst.*, vol. 12, no. 9, p. 125, 5772, doi: 10.5772/61236.

[14] K. Kuru, D. Ansell, W. Khan, and H. Yetgin, "Analysis and optimization of unmanned aerial vehicle swarms in logistics: An intelligent delivery platform," *IEEE Access*, vol. 7, pp. 15804–15831, 2019.

[15] K. Kuru, "Planning the future of smart cities with swarms of fully autonomous unmanned aerial vehicles using a novel framework," *IEEE Access*, vol. 9, pp. 6571–6595, 2021.

[16] K. Kuru, D. Ansell, D. Jones, B. Watkinson, J. M. Pinder, J. A. Hill, E. Muzzall, C. Tinker-Mill, K. Stevens, and A. Gardner, "Intelligent airborne monitoring of livestock using autonomous uninhabited aerial vehicles," in *Proc. 11th Eur. Conf. Precision Livestock Farming*, 2024, pp. 1100–1110.

[17] K. Kuru, J. M. Pinder, B. J. Watkinson, D. Ansell, K. Vinning, L. Moore, C. Gilbert, A. Sujit, and D. Jones, "Toward mid-air collision-free trajectory for autonomous and pilot-controlled unmanned aerial vehicles," *IEEE Access*, vol. 11, pp. 100323–100342, 2023.

[18] K. Kuru, S. Clough, D. Ansell, J. McCarthy, and S. McGovern, "Intelligent airborne monitoring of irregularly shaped man-made marine objects using statistical machine learning techniques," *Ecol. Informat.*, vol. 78, Dec. 2023, Art. no. 102285.

[19] K. Kuru, S. Clough, D. Ansell, J. McCarthy, and S. McGovern, "WILDetect: An intelligent platform to perform airborne wildlife census automatically in the marine ecosystem using an ensemble of learning techniques and computer vision," *Expert Syst. Appl.*, vol. 231, Nov. 2023, Art. no. 120574.

[20] A. Nikulin, T. S. De Smet, J. Baur, W. D. Frazer, and J. C. Abramowitz, "Detection and identification of remnant PFM-1 'butterfly mines' with a UAV-based thermal-imaging protocol," *Remote Sens.*, vol. 10, no. 11, p.1672, Oct. 2018, doi: 10.3390/rs10111672.

[21] L. He, S. Ji, W. R. Scott, and L. Carin, "Adaptive multimodality sensing of landmines," *IEEE Trans. Geosci. Remote Sens.*, vol. 45, no. 6, pp. 1756–1774, Jun. 2007.

[22] V. Kovalenko, A. G. Yarovoy, and L. P. Ligthart, ‘‘A novel clutter suppression algorithm for landmine detection with GPR,’’ *IEEE Trans. Geosci. Remote Sens*., vol. 45, no. 11, pp. 3740–3751, Oct. 2007.

[23] Y. Sun and J. Li, ‘‘Adaptive learning approach to landmine detection,’’ *IEEE Trans. Aerosp. Electron. Syst*., vol. 41, no. 3, pp. 973–985, Jul. 2005.

[24] M. G. Fernández, G. Á. Narciandi, A. Arboleya, C. V. Antuña, F. L. Andrés, and Y. Á. López, ‘‘Development of an airborne-based GPR system for landmine and IED detection: Antenna analysis and intercomparison,’’ *IEEE Access*, vol. 9, pp. 127382–127396, 2021.

[25] T. W. Du Bosq, J. M. Lopez-Alonso, and G. D. Boreman, ‘‘Millimeter wave imaging system for land mine detection,’’ *Appl. Opt*., vol. 45, no. 22, p. 5686, Aug. 2006.

[26] K. Stone, J. Keller, K. C. Ho, M. Busch, and P. D. Gader, ‘‘On the registration of FLGPR and IR data for a forward-looking landmine detection system and its use in eliminating FLGPR false alarms,’’ *Proc. SPIE*, vol. 6953, pp. 331–342, Apr. 2008, doi: 10.1117/12.782238.

[27] M. Garcia-Fernandez, A. Morgenthaler, Y. Alvarez-Lopez, F. L. Heras, and C. Rappaport, ‘‘Bistatic landmine and IED detection combining vehicle and drone mounted GPR sensors,’’ *Remote Sens*., vol. 11, no. 19, p. 2299, Oct. 2019. [Online]. Available: https://www.mdpi.com/2072-4292/11/19/2299

[28] M. García-Fernández, G. Álvarez-Narciandi, Y. Á. López, and F. L.-H. Andrés, ‘‘Improvements in GPR-SAR imaging focusing and detection capabilities of UAV-mounted GPR systems,’’ *ISPRS J. Photogramm. Remote Sens*., vol. 189, pp. 128–142, Jul. 2022.[Online]. Available: https://www.sciencedirect.com/science/article/pii/S0924271622001113

[29] D. íipo≤ and D. Gleich, ‘‘A lightweight and low-power UAV-borne ground penetrating radar design for landmine detection,’’ *Sensors,* vol. 20, no. 8, p. 2234, Apr. 2020. [Online]. Available: https://www.mdpi.com/1424-8220/20/8/2234

[30] J. Ishikawa, K. Furuta, and N. Pavkovi, ‘‘Test and evaluation of Japanese GPR-EMI dual sensor systems at the Benkovac test site in Croatia,’’ in *Anti-Personnel Landmine Detection for Humanitarian Demining: The Current Situation and Future Direction for Japanese Research and Development*. London, U.K.: Springer, 2009, pp. 63–81, doi: 10.1007/978-1-84882-346-4_5.

[31] D. Donskoy, A. Ekimov, N. Sedunov, and M. Tsionskiy, ‘‘Nonlinear seismo-acoustic land mine detection and discrimination,’’ *J. Acoust. Soc. Amer*., vol. 111, no. 6, pp. 2705–2714, 2002, doi: 10.1121/1.1477930.

[32] K. Kuru and H. Yetgin, ‘‘Transformation to advanced mechatronics sys-tems within new industrial revolution: A novel framework in automation of everything (AoE),’’ *IEEE Access*, vol. 7, pp. 41395–41415, 2019.

[33] K. Kuru, ‘‘Management of geo-distributed intelligence: Deep insight as a service (DINSaaS) on forged cloud platforms (FCP),’’ *J. Parallel Distrib. Comput*., vol. 149, pp. 103–118, Mar. 2021.

[34] N. T. Thnh, H. Sahli, and D. N. Ho, ‘‘Finite-difference methods and validity of a thermal model for landmine detection with soil property estimation,’’ *IEEE Trans. Geosci. Remote Sens*., vol. 45, no. 3, pp. 656–674, Mar. 2007.

[35] J. M. Bioucas-Dias, A. Plaza, G. Camps-Valls, P. Scheunders, N. Nasrabadi, and J. Chanussot, ‘‘Hyperspectral remote sensing data analysis and future challenges,’’ *IEEE Geosci. Remote Sens. Mag.*, vol. 1, no. 2, pp. 6–36, Jun. 2013.

[36] M. J. Khan, H. S. Khan, A. Yousaf, K. Khurshid, and A. Abbas, ‘‘Modern trends in hyperspectral image analysis: A review,’’ *IEEE Access*, vol. 6, pp. 14118–14129, 2018.

[37] A. Banerji and J. Goutsias, ‘‘A morphological approach to automatic mine detection problems,’’ *IEEE Trans. Aerosp. Electron. Syst*., vol. 34, no. 4, pp. 1085–1096, Oct. 1998.

[38] J. M. M. Anderson, ‘‘A generalized likelihood ratio test for detecting land mines using multispectral images,’’ *IEEE Geosci. Remote Sens. Lett.*, vol. 5, no. 3, pp. 547–551, Jul. 2008.

[39] N. T. Thanh, H. Sahli, and D. N. Hao, ‘‘Infrared thermography for buried landmine detection: Inverse problem setting,’’ *IEEE Trans. Geosci. Remote Sens*., vol. 46, no. 12, pp. 3987–4004, Dec. 2008.

[40] M. G. Fernández, Y. Á. López, A. A. Arboleya, B. G. Valdés, Y. R. Vaqueiro, F. L.-H. Andrés, and A. P. García, ‘‘Synthetic aperture radar imaging system for landmine detection using a ground penetrating radar on board a unmanned aerial vehicle,’’ *IEEE Access*, vol. 6, pp. 45100–45112, 2018.

[41] M. Garcia-Fernandez, Y. Alvarez-Lopez, and F. L. Heras, ‘‘Autonomous airborne 3D SAR imaging system for subsurface sensing: UWB-GPR on board a UAV for landmine and IED detection,’’ *Remote Sens*., vol. 11, no. 20, p. 2357, Oct. 2019. [Online]. Available: https://www.mdpi.com/2072-4292/11/20/2357

[42] M. Schartel, R. Burr, R. Bähnemann, W. Mayer, and C. Waldschmidt, ‘‘An experimental study on airborne landmine detection using a circular synthetic aperture radar,’’ 2005, *arXiv:2005.02600*.

[43] M. García-Fernández, Y. Á. López, and F. L. Andrés, "Airborne multi-channel ground penetrating radar for improvised explosive devices and landmine detection," *IEEE Access*, vol. 8, pp. 165927–165943, 2020.

[44] Precedence Research. (2024). *Magnetometer Market Size, Share, and Trends 2024 To 2034*. [Online]. Available: https:// www. precedenceresearch. com/magnetometer-market

[45] H. Liu, C. Zhao, J. Zhu, J. Ge, H. Dong, Z. Liu, and N. Mrad, "Active detection of small UXO-like targets through measuring electromagnetic responses with a magneto-inductive sensor array," *IEEE Sensors J.*, vol. 21, no. 20, pp. 23558–23567, Oct. 2021.

[46] H. Huang and I. J. Won, "Characterization of UXO-like targets using broadband electromagnetic induction sensors," *IEEE Trans. Geosci. Remote Sens.*, vol. 41, no. 3, pp. 652–663, Mar. 2003.

[47] A. M. Elsayad, F. Mubarak, H. Abdullah, M. Fahhad, and N. Saad, "Advancements in passive landmine detection a multiclass approach with fluxgate sensor and machine learning models," in *Proc. 41st Nat. Radio Sci. Conf. (NRSC)*, Apr. 2024, pp. 158–165.

[48] Y. Zhang, X. Liao, and L. Carin, "Detection of buried targets via active selection of labeled data: Application to sensing subsurface UXO," *IEEE Trans. Geosci. Remote Sens.*, vol. 42, no. 11, pp. 2535–2543, Nov. 2004.

[49] Y. Mu, L. Chen, and Y. Xiao, "Small signal magnetic compensation method for UAV-borne vector magnetometer system," *IEEE Trans. Instrum. Meas.*, vol. 72, pp. 1–7, 2023.

[50] H. Lee, C. Lee, H. Jeon, J. J. Son, Y. Son, and S. Han, "Interference-compensating magnetometer calibration with estimated measurement noise covariance for application to small-sized UAVs," *IEEE Trans. Ind. Electron.*, vol. 67, no. 10, pp. 8829–8840, Oct. 2020.

[51] L.-S. Yoo, J.-H. Lee, Y.-K. Lee, S.-K. Jung, and Y. Choi, "Application of a drone magnetometer system to military mine detection in the demilitarized zone," *Sensors*, vol. 21, no. 9, p. 3175, May 2021. [Online]. Available: https:// www.mdpi.com/1424-8220/21/9/3175

[52] L.-S. Yoo, J.-H. Lee, S.-H. Ko, S.-K. Jung, S.-H. Lee, and Y.- K. Lee, "A drone fitted with a magnetometer detects landmines," *IEEE Geosci. Remote Sens. Lett.*, vol. 17, no. 12, pp. 2035–2039, Dec. 2020.

[53] A. Barnawi, N. Thakur, N. Kumar, K. Kumar, B. Alzahrani, and A. Almansour, "Classification of area of interest based on 2D map using segmentation for path planning of airborne landmines detection," in *Proc. IEEE Int. Conf. Consum. Electron. (ICCE)*, Jan. 2023, pp. 1–6.

[54] K. Kuru, D. Ansell, M. Jones, C. De Goede, and P. Leather, "Feasibility study of intelligent autonomous determination of the bladder voiding need to treat bedwetting using ultrasound and smartphone ML techniques: Intelligent autonomous treatment of bedwetting," *Med. Biol. Eng. Comput.*, vol. 57, no. 5, pp. 1079–1097, Dec. 2018, doi: 10.1007/s11517-018-1942-9.

[55] K. Kuru, D. Ansell, M. Jones, B. J. Watkinson, N. Caswell, P. Leather, A. Lancaster, P. Sugden, E. Briggs, C. Davies, T. C. Oh, K. Bennett, and C. De Goede, "Intelligent autonomous treatment of bedwetting using non-invasive wearable advanced mechatronics systems and MEMS sensors: Intelligent autonomous bladder monitoring to treat NE," *Med. Biol. Eng. Comput.*, vol. 58, no. 5, pp. 943–965, Feb. 2020, doi: 10.1007/s11517-019-02091-x.

[56] K. Kuru, D. Ansell, D. Hughes, B. J. Watkinson, F. Gaudenzi, M. Jones, D. Lunardi, N. Caswell, A. R. Montiel, P. Leather, D. Irving, K. Bennett, C. McKenzie, P. Sugden, C. Davies, and C. Degoede, "Treatment of nocturnal enuresis using miniaturised smart mechatronics with artificial intelligence," *IEEE J. Transl. Eng. Health Med.*, vol. 12, pp. 204–214, 2024.

[57] N. Caswell, K. Kuru, D. Ansell, M. J. Jones, B. J. Watkinson, P. Leather, A. Lancaster, P. Sugden, E. Briggs, C. Davies, C. Oh, K. Bennett, and C. DeGoede, "Patient engagement in medical device design: Refining the essential attributes of a wearable, pre-void, ultrasound alarm for nocturnal enuresis," *Pharmaceutical Med.*, vol. 34, no. 1, pp. 39–48, Jan. 2020, doi: 10.1007/s40290-019-00324-w.

[58] K. Kuru, "Sensors and sensor fusion for decision making in autonomous driving and vehicles," Univ. Central Lancashire, Preston, U.K., Rep. 37342, 2023.

[59] K. Kuru, D. Ansell, D. Jones, B. Watkinson, J. M. Pinder, J. A. Hill, E. Muzzall, C. Tinker-Mill, K. Stevens, and A. Gardner, "IoTFaUAV: Intelligent remote monitoring of livestock in large farms using autonomous unmanned aerial vehicles with vision-based sensors," *Biosyst. Eng.*, 2024.

[60] K. Kuru, D. Ansell, and D. Jones, "Airborne vision-based remote sensing imagery datasets from large farms using autonomous drones for monitoring livestock," Univ. Central Lancashire, Preston, U.K., Rep. 49526, 2023.

[61] K. Kuru, S. Worthington, D. Ansell, J. M. Pinder, B. Watkinson, D. Jones, and C. Tinker-Mill, "Platform to test and evaluate human-in-the-loop telemanipulation schemes for autonomous unmanned aerial systems," in *Proc. 20th IEEE/ASME Int. Conf. Mech. Embedded Syst. Appl. (MESA)*, Sep. 2024, pp. 1–8.

[62] K. Kuru, S. Worthington, D. Ansell, J. M. Pinder, A. Sujit, B. Watkinson, K. Vinning, L. Moore, C. Gilbert, D. Jones, and C. Tinker-Mill, "AITL-WING-HITL: Telemanipulation of autonomous drones using digital twins of aerial traffic interfaced with wing," *Robot. Auto. Syst.*, vol. 180, 2024.

[63] K. Kuru and D. Ansell, "Vision-based remote sensing imagery datasets from Benkovac landmine test site using an autonomous drone for detecting landmine locations," Univ. Central Lancashire, Preston, U.K., Rep. 49065, 2023.

[64] J. Jirigalatu, V. Krishna, E. L. S. da Silva, and A. Døssing, "Experiments on magnetic interference for a portable airborne magnetometry system using a hybrid unmanned aerial vehicle (UAV)," *Geosci. Instrum., Methods Data Syst.*, vol. 10, no. 1, pp. 25–34, Jan. 2021. [Online]. Available: https://gi.copernicus.org/articles/10/25/2021/

[65] L. E. Tuck, C. Samson, J. Laliberté, and M. Cunningham, "Magnetic interference mapping of four types of unmanned aircraft systems intended for aeromagnetic surveying," *Geosci. Instrum., Methods Data Syst.*, vol. 10, no. 1, pp. 101–112, May 2021. [Online]. Available: https://gi.copernicus.org/articles/10/101/2021/

[66] O. Maidanyk, Y. Meleshko, and S. Shymko, "Study of influence of quadrocopter design and settings on quality of its work during monitoring of ground objects," *Adv. Inf. Syst.*, vol. 5, no. 4, pp. 64–69, Dec. 2021, doi: 10.20998/2522-9052.2021.4.10.

[67] K. Kuru, "Magnetic field mapping of a landmine field using a magnetometer-integrated drone and intelligent application," Univ. Central Lancashire, Preston, U.K., Rep. 49066, 2024, doi: 10.21227/ebny-b828.

[68] K. Kuru and W. Khan, "Novel hybrid object-based non-parametric clustering approach for grouping similar objects in specific visual domains," *Appl. Soft Comput.*, vol. 62, pp. 667–701, Jan. 2018. [Online]. Available: https://www.sciencedirect.com/science/article/pii/S156849461 7306701

[69] N. Walsh and W. Walsh, "Rehabilitation of landmine victims—The ultimate challenge," *Bull. World Health Org.*, vol. 81, pp. 665–670, Feb. 2003.

[70] S. Pati, B. K. Mishra, S. K. Bishnu, A. Mukhopadhyay, and A. Chakraborty, "DroneMag: A novel approach using drone technology for detection of magnetic metal," in *Proc. 7th Int. Conf. Electron., Mater. Eng. Nano-Technol. (IEMENTech)*, Dec. 2023, pp. 1–4. [Online]. Available: https://api.semanticscholar.org/CorpusID:267576190

[71] C. Yilmaz, H. T. Kahraman, and S. Söyler, "Passive mine detection and classification method based on hybrid model," *IEEE Access*, vol. 6, pp. 47870–47888, 2018.

[72] K. Kuru, O. Erogul, and C. Xavier, "Autonomous low power monitoring sensors," *Sensors*, vol. 21, pp. 1–2, Aug. 2021.

Originally published in IEEE Access, VOLUME 12, 2024. Republished with authors' permission.

Latest eBee VISION application software

AgEagle Aerial Systems has introduced version 2.1.0 of its eBee VISION application software, designed to significantly enhance UAV capabilities. The update expands the system's functionality, introducing circular and grid mapping features. It can continue missions in GNSS-denied environments and allows manual deactivation of GNSS to prevent jamming or spoofing. It implements the STANAG 4609 standard, the official format for motion imagery exchange within the NATO nations. This involves embedding UAV position and camera information into the videos recorded by the UAV and those broadcasted by the Ground Control Station. *ageagle.com*

DroneDeploy and GEODNET partnership

DroneDeploy has entered a strategic partnership with the GEODNET Foundation to enhance enterprise UAV capabilities by providing access to high-precision positioning data. The partnership will grant DroneDeploy customers access to GEODNET's extensive network of 10,000 registered stations. The agreement also includes provisions for DroneDeploy to work with its users to establish additional GEODNET stations in areas currently lacking coverage, further expanding the network's reach. *www.dronedeploy.com*

"Drone in a Box" enterprise solution

DJI has launched DJI Dock 3 -"Drone in a Box" solution that supports vehicle mounting, empowering 24/7 remote operations for various environments. It comes with the all-new DJI Matrice 4D or DJI Matrice 4TD drone. It can operate and charge seamlessly in extreme temperatures up to 50°C (122°F) and as low as -30°C (-22°F) when pre-heated. Its design further safeguards its internal system with IP56 dust and water-resistant rating. *www.dji.com*

UAV Navigation introduces 3D Geocaging for autopilots

UAV Navigation introduced a new 3D Geocaging feature for its autopilot systems, aimed at enhancing flight safety and efficiency for UAVs. This functionality autonomously ensures that an aircraft remains within a designated three-dimensional volume, preventing it from straying into restricted airspace or hazardous areas. The feature improves situational awareness and operational control, making it a valuable tool for both commercial and defense applications. *www.uavnavigation.com*

GNSS Constellation Specific Monthly Analysis Summary: February 2025

The analysis performed in this report is solely his work and own opinion. State Program: U.S.A (G); EU (E); China (C) "Only MEO- SECM satellites"; Russia (R); Japan (J); India (I)

Narayan Dhital
Actively involved to support international collaboration in GNSS-related activities. He has regularly supported and contributed to different workshops of the International Committee on GNSS (ICG), and the United Nations Office for Outer Space Affairs (UNOOSA). As a professional employee, the author is working as GNSS expert at the Galileo Control Center, DLR GfR mbH, Germany.

Introduction

The article is a continuation of monthly performance analysis of the GNSS constellation. Please refer to previous issues for past analysis. Regarding applications, a short overview on the satellite control to maintain the attitude of GNSS satellites with respect to the mission requirement is provided. The implications on the precise use cases are also highlighted.

Analyzed Parameters for February 2025

(**Dhital et. al, 2024**) provides a brief overview of the necessity and applicability of monitoring the satellite clock and orbit parameters.

a. Satellite Broadcast Accuracy, measured in terms of **Signal-In-Space Range Error (SISRE) (Montenbruck et. al, 2010)**.

b. SISRE-Orbit (only orbit impact on the range error), SISRE (both orbit and clock impact), and SISRE-PPP (as seen by the users of carrier phase signals, where the ambiguities absorb the unmodelled biases related to satellite clock and orbit estimations. Satellite specific clock bias is removed) (Hauschlid et.al, 2020)

c. Clock Discontinuity: The jump in the satellite clock offset between two consecutive batches of data uploads from the ground mission segment. It is indicative of the quality of the satellite atomic clock and associated clock model.

d. URA: User Range Accuracy as an indicator of the confidence on the accuracy of satellite ephemeris. It is mostly used in the integrity computation of RAIM.

e. GNSS-UTC offset: It shows stability of the timekeeping of each constellation w.r.t the UTC

f. Satellite Attitude Quaternions: The optimal control of the GNSS satellite attitude is mission critical and the awareness of the orientation of the satellites is important for the user level PVT solutions. Quaternions are used to represent the attitude of the GNSS satellites.

(a), (b) Satellite Clock and Orbit Accuracy (monthly RMS values)

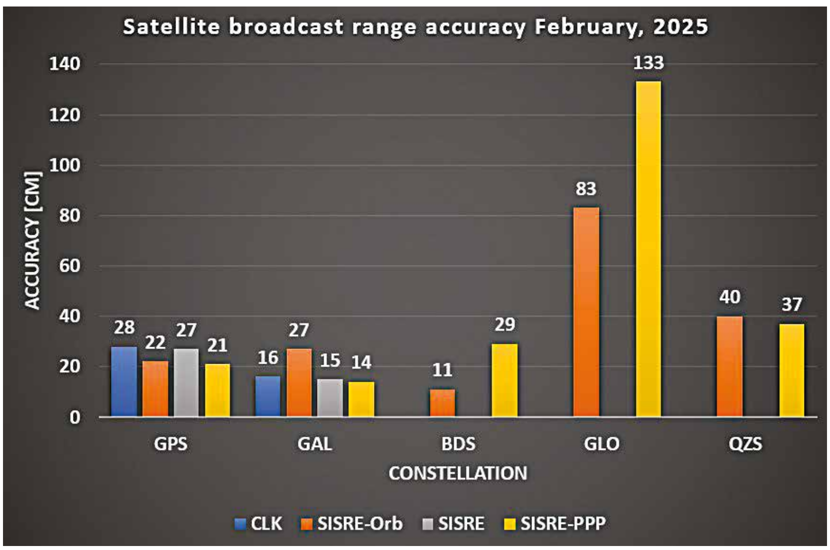

Note:- for India's IRNSS there are no precise satellite clocks and orbits as they broadcast only 1 frequency which does not allow the dual frequency combination required in precise clock and orbit estimation; as such, only URA and Clock Discontinuity is analyzed.

(c)-1 Satellite Clock Jump per Mission Segment Upload

Const	Mean [ns]	Max [ns]	95_Percentile [ns]	99_Percentile [ns]	Remark (Best and Worst 95 %)
IRNSS	×	×	×	×	×
GPS	×	×	×	×	×
GAL	×	×	×	×	×

Due to data glitches, the satellite clock jump statistics are not provided for this month. The processing will be recovered and provided together with the month of March.

On a positive side, a brief overview on the satellite atomic clock stability of the newly operational Galileo satellites GSAT0232 GSAT0226 (PRNs: E16 and E23) are provided. As it can be seen in the plot below (based on the 24 hours data on the 14th of February, 2025), the Passive Hydrogen Maser (PHM) clocks of both satellites behave as expected. The PHM of other Galileo satellites, including the E06 and E29 that were launched in 2024 as well, are provided as references. The relatively poor stability of RFS clock in satellites E11 and 19 are also shown.

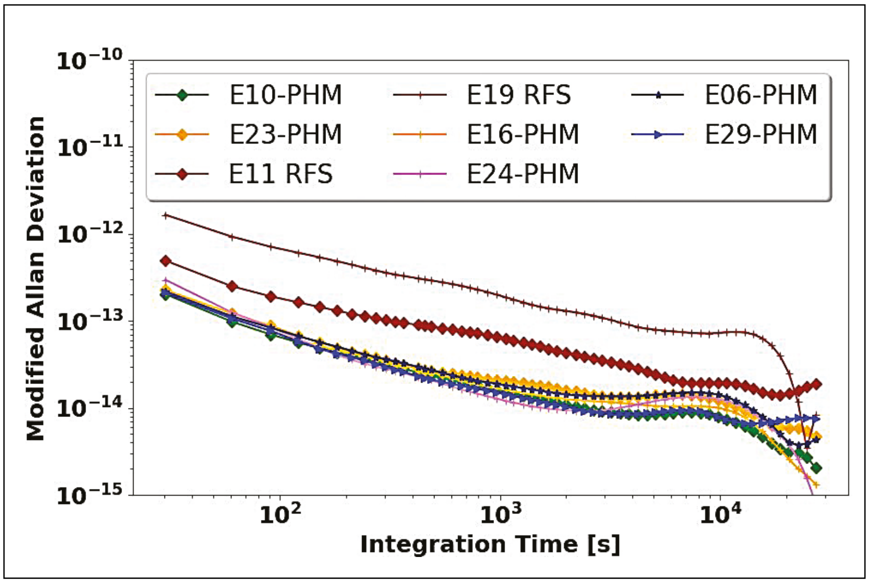

(d) User Range Accuracy (Number of Occurrences in Broadcast Data 01-31 January)

IRNSS-SAT	2 [m]	2.8 [m]	4.0 [m]	5.7 [m]	8 [m]	8192 [m]	9999.9	Remark Other URA values (frequency)
I02	2671	42	-	-	2	-	-	-
I03	-	-	-	-	-	-	-	-
I06	2688	16	2	-	4	-	2	16 (1), 11.3 (1), 32 (1)
I09	431	8	1	-	1	-	-	-
I10	529	2	1	-	2	-	-	-

(f) Satellite Attitude Quaternions

The inertial attitude of a GNSS satellite is determined by the mission requirement to point the navigation antenna towards the Earth while keeping the solar panels optimally towards the Sun. As a result, the satellite control mechanism continuously rotates the satellite around the Earth-pointing axis, ensuring the solar panel axis remains perpendicular to the Sun's direction. This method is known as the Yaw Steering (YS) attitude control. However, this mode requires rapid yaw-slews of up to 180 degrees when the Sun is near the orbital plane. In such cases, an orbit normal (ON) mode is often preferred, where the satellite body is fixed in the local orbital frame and the solar panel rotation axis is kept perpendicular to the orbital plane. The ON is also applied for the Geostationary satellites. Figure F(a) shows the sketch of YS and ON mode adopted from (**Guo et.al, 2017**). (**Montenbruck et.al, 2015**) provides detail on the attitude of the satellites relating the body-reference frame and orbit plane. When satellites enter noon maneuver or shadow crossing regimes, their actual attitudes can deviate from nominal values. Improper attitude models can lead to errors due to the wind-up effect and satellite antenna Phase Center Offset (PCO), deteriorating positioning accuracy. While the improvement in modeled attitude for multi-GNSS solutions might be modest, it can be significant for single positioning and in urban areas with limited satellite tracking.

The Euler angles that represent the rotation of the satellite suffers from the gimble lock and singularities, where two of the three axis aligns rendering loss of the degree of freedom. The use of quaternions overcome that problem and is also efficient for representing the attitudes. The satellite attitude quaternions $q = (q_0, q_1, q_2, q_3)$ are provided by IGS ACs to ensure consistency in the attitude model used by both the network and user end. These quaternions describe the transformation between the Terrestrial Frame and the Satellite Body-Frame, ensuring accurate positioning.

(e) GNSS-UTC Offset

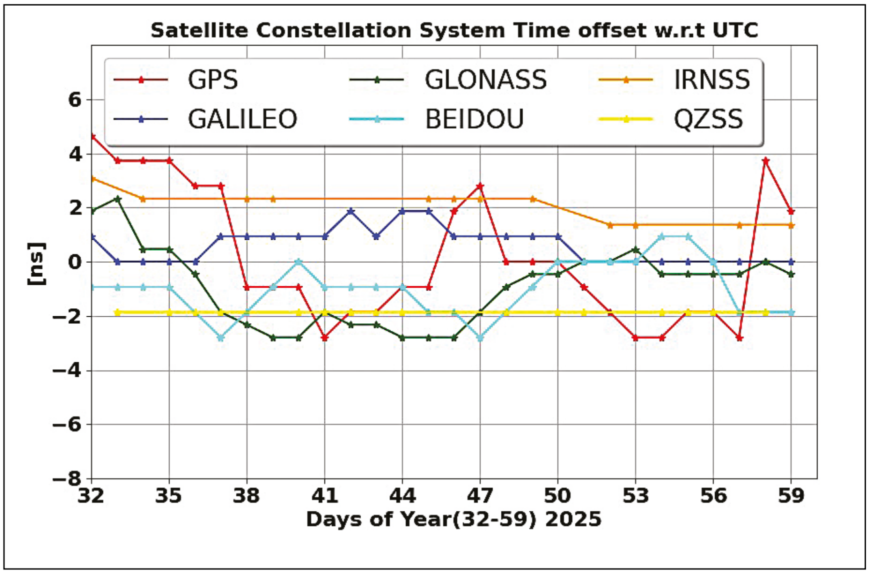

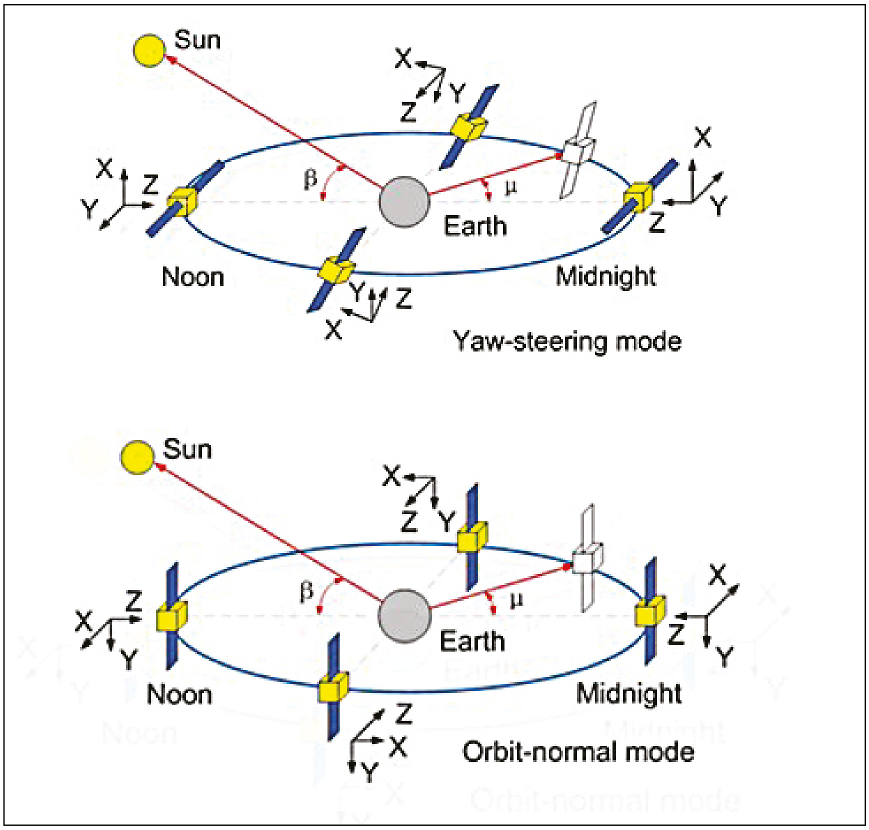

Figure F 1: The orientation of the satellite maximizing the solar panel exposure to the Sun direction and keeping the antenna pointed towards the Earth gives yaw steering attitude control (Top). The orientation of the satellite panels in perpendicular to the orbit plan gives the orbit normal attitude control (bottom).

From the user end, applying the attitude quaternions allows the computation of the X, Y, and Z axis unit vectors of the satellite Body-Fixed Frame (BFS) as follows

Given: $q = (q_0, q_1, q_2, q_3)$ from quaternion files and $q_0^2 + q_1^2 + q_2^2 + q_3^2 = 1$. Then,

$$e_x = \begin{bmatrix} q_0^2 + q_1^2 - q_2^2 - q_3^2 \\ 2\cdot(q_1q_2 - q_0q_3) \\ 2\cdot(q_1q_3 + q_0q_2) \end{bmatrix}$$

$$e_y = \begin{bmatrix} 2\cdot(q_1q_2 + q_0q_3) \\ q_0^2 - q_1^2 + q_2^2 - q_3^2 \\ 2\cdot(q_2q_3 - q_0q_1) \end{bmatrix}$$

$$e_z = \begin{bmatrix} 2\cdot(q_1q_3 - q_0q_2) \\ 2\cdot(q_2q_3 + q_0q_1) \\ q_0^2 - q_1^2 - q_2^2 + q_3^2 \end{bmatrix}$$

Here e_x, e_y, e_z represented the body-fixed frame unit vectors.

In the generic form, the transformation between the body frame and the terrestrial frame is given by:

$$(0, x_1, x_2, x_3) = q \cdot (0, X_1, X_2, X_3) \cdot \bar{q}$$

Where $\bar{q}$ is the transposed quaternion.

The use of this relationship allows for easy computation of the satellite's Phase Center in the terrestrial frame using the Center of Mass (CoM) position from the sp3 files and the Phase Center Offsets (PCO) vector from the ANTEX file:

$$Phase\ Center_{Earth} = CoM_{Earth} + \bar{q} \cdot (0, \overrightarrow{PCO}) \cdot q$$

This ensures accurate positioning and minimizes errors due to the wind-up effect and PCO (**IGS et.al, 2019**)

Such implementation in the user algorithm that ingest the attitude quaternions provided by the ACs improves the PVT solution. It is not envisaged to demonstrate in this article and viewers are referred to (**Yuang et.al, 2025**) for relevant analysis. However, a short demonstration on the usability of the attitude quaternions to understand the behavior of various satellites in different orbits is provided in Figure F 2.

The computed angle as shown in the y-axis is with respect to the satellite body frame (nadir pointing vector and the along track vector). It is not based on the orbit reference frame which explains the offset of the yaw angle. However, the evolution of the yaw behavior for the 24 hours is explainable through the computed angle. The distinct evolution is seen for J07 and

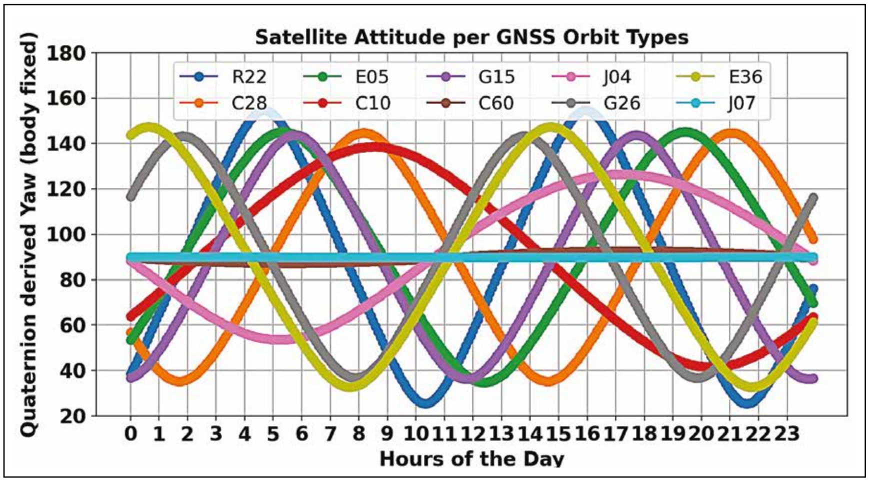

Figure F 2: The behavior of the satellite attitude dictated by the yaw angle (derived with quaternions with respect to the body fixed frame). The time is 24 hours on the 14th of February 2025. The satellites are denoted by the GNSS letter and the PRN numbers. C10 and J04 are IGSO following YS mode; C60 and J07 are GEO following ON mode and remaining satellites are MEO following YS mode too.

C60 which are the Geostationary satellites that follow the orbit normal attitude control of the satellite. Similarly, the IGSO based satellites (C10 and J04) show varying yaw angle with slow change as the orbit period is close to 24 hours while the MEO based satellites show 2 cycles of varying yaw angles per 24 hours matching the orbit period close to 12 hours. The behavior of the satellite attitude in the shadow crossing and low beta angle (angle of the orbit plan with respect to the Sun direction) period was provided in previous months analysis (February-March 2024).

Monthly Performance Remarks:

1. Satellite Clock and Orbit Accuracy:
   - The performance of all constellations is relatively stable and unchanged from previous month.
   - The data glitch in the computation prevented the analysis of the satellite clock jump. However, an overview on the newly operational Galileo satellite clocks (E16 and E23) was provided. The stability of the PHM of E16 and E23 looks as expected.
   - The URA for I06 showed a little more scatter in comparison to previous months.
2. UTC Prediction (GNSS-UTC):
   - All constellations show stable UTC prediction with minor variations. It is showing a good consistency in last months.

References

Alonso M, Sanz J, Juan J, Garcia, A, Casado G (2020) Galileo Broadcast Ephemeris and Clock Errors Analysis: 1 January 2017 to 31 July 2020, MDPI

Alonso M (2022) Galileo Broadcast Ephemeris and Clock Errors, and Observed Fault Probabilities for ARAIM, Ph.D Thesis, UPC

Bento, M (2013) Development and Validation of an IMU/GPS/Galileo Integration Navigation System for UAV, PhD Thesis, UniBW.

BIMP (2024 a) https://e-learning.bipm.org/pluginfile.php/6722/mod_label/intro/User_manual_cggtts_analyser.pdf?time=1709905608656

BIMP (2024 b) https://e-learning.bipm.org/mod/folder/view.php?id=1156&forceview=1

BIMP (2024 c) https://cggtts-analyser.streamlit.app

Bruggemann, Troy & Greer, Duncan & Walker, R.. (2011). GPS fault detection with IMU and aircraft dynamics. IEEE Transactions on Aerospace and Electronic Systems - IEEE TRANS AEROSP ELECTRON SY. 47. 305-316. 10.1109/TAES.2011.5705677.

Cao X, Zhang S, Kuang K, Liu T (2018) The impact of eclipsing GNSS satellites on the precise point positioning, Remote Sensing 10(1):94

Chen, K., Chang, G. & Chen, C (2021) GINav: a MATLAB-based software for the data processing and analysis of a GNSS/IMU integrated navigation system. *GPS Solut* **25**, 108. https://doi.org/10.1007/s10291-021-01144-9

Curran, James T. & Broumendan, Ali. (2017). On the use of Low-Cost IMUs for GNSS Spoofing Detection in Vehicular Applications.

Dhital N (2024) GNSS constellation specific monthly analysis summary, Coordinates, Vol XX, Issue 1, 2, 3, 4

Dhital N (2025) GNSS constellation specific monthly analysis summary, Coordinates, Vol XXI, Issue 1

GINAv (2025). https://geodesy.noaa.gov/gps-toolbox/GINav.shtml

Goercke, L (2017) GNSS-denied navigation of fixed-wing aircraft using low-cost sensors and aerodynamic motion models, PhD Thesis, TUM.

Guo F, Zhang X, Wang J (2015) Timing group delay and differential code bias corrections for BeiDou positioning, J Geod,

Hauschlid A, Montenbruck O (2020) Precise real-time navigation of LEO satellites using GNSS broadcast ephemerides, ION

IERS C04 (2024) https://hpiers.obspm.fr/iers/eop/eopc04/eopc04.1962-now

IGS (2021) RINEX Version 4.00 https://files.igs.org/pub/data/format/rinex_4.00.pdf

Kj, Nirmal & Sreejith, A. & Mathew, Joice & Sarpotdar, Mayuresh & Suresh, Ambily & Prakash, Ajin & Safonova, Margarita & Murthy, Jayant. (2016). Noise modeling and analysis of an IMU-based attitude sensor: improvement of performance by filtering and sensor fusion. 99126W. 10.1117/12.2234255.

Li M, Wang Y, Li W (2023) performance evaluation of real-time orbit determination for LUTAN-01B satellite using broadcast earth orientation parameters and multi-GNSS combination, GPS Solutions, Vol 28, article number 52

Li W, Chen G (2023) Evaluation of GPS and BDS-3 broadcast earth rotation parameters: a contribution to the ephemeris rotation error Montenbruck

Liu, Yue & Liu, Fei & Gao, Yang & Zhao, Lin. (2018). Implementation and Analysis of Tightly Coupled Global Navigation Satellite System Precise Point Positioning/Inertial Navigation System (GNSS PPP/IMU) with IMUfficient Satellites for Land Vehicle Navigation. Sensors. 18. 4305. 10.3390/s18124305.

O, Steigenberger P, Hauschlid A (2014) Broadcast versus precise ephemerides: a multi-GNSS perspective, GPS Solutions

Liu T, Chen H, Jiang Weiping (2022) Assessing the exchanging satellite attitude quaternions from CNES/CLS and their application in the deep eclipse season, GPS Solutions 26(1)

Montenbruck O, Steigenberger P, Hauschlid A (2014) Broadcast versus precise ephemerides: a multi-GNSS perspective, GPS Solutions

Montenbruck O, Hauschlid A (2014 a) Differential Code Bias Estimation using Multi-GNSS Observations and Global Ionosphere Maps, ION

Niu, Z.; Li, G.; Guo, F.; Shuai, Q.; Zhu, B (2022) An Algorithm to Assist the Robust Filter for Tightly Coupled RTK/IMU Navigation System. *Remote Sens.* **2022**, *14*, 2449. https://doi.org/10.3390/rs14102449

Schmidt, G, Phillips, R (2010) IMU/GPS Integration Architecture Performance Comparisons. NATO.

Steigenberger P, Montenbruck O, Bradke M, Ramatschi M (2022) Evaluation of earth rotation parameters from modernized GNSS navigation messages, GPS Solutions 26(2)

Suvorkin, V., Garcia-Fernandez, M., González-Casado, G., Li, M., & Rovira-Garcia, A. (2024). Assessment of Noise of MEMS IMU Sensors of Different Grades for GNSS/IMU Navigation. *Sensors*, *24*(6), 1953. https://doi.org/10.3390/s24061953

Sylvain L, Banville S, Geng J, Strasser S (2021) Exchanging satellite attitude quaternions for improved GNSS data processing consistency, Vol 68, Issue 6, pages 2441-2452

Tanil, Cagatay & Khanafseh, Samer & Pervan, Boris. (2016). An IMU Monitor agaIMUt GNSS Spoofing Attacks during GBAS and SBAS-assisted Aircraft Landing Approaches. 10.33012/2016.14779.

Walter T, Blanch J, Gunning K (2019) Standards for ARAIM ISM Data Analysis, ION

Wang, C & Jan, S (2025). Performance Analysis of MADOCA-Enhanced Tightly Coupled PPP/IMU. NAVIGATION: Journal of the IMUtitute of Navigation March 2025, 72 (1) navi.678; DOI: https://doi.org/10.33012/navi.678

Wang N, Li Z, Montenbruck O, Tang C (2019) Quality assessment of GPS, Galileo and BeiDou-2/3 satellite broadcast group delays, Advances in Space Research

Wang J, Huang S, Lia C (2014) Time and Frequency Transfer System Using GNSS Receiver, Asia-Pacific Radio Science, Vol 49, Issue 12

https://cggtts-analyser.streamlit.app

Yang N, Xu A, Xu Z, Xu Y, Tang L, Li J, Zhu H (2025) Effect of WHU/GFZ/CODE satellite attitude quaternion products on the GNSS kinematic PPP during the eclipse season, Advances in Space Research, Volume 75, Issue 1,

Note: References in this list might also include references provided to previous issues.

Data sources and Tools:

https://cddis.nasa.gov (Daily BRDC); http://ftp.aiub.unibe.ch/CODE_MGEX/CODE/ (Precise Products); BKG “SSRC00BKG” stream; IERS C04 ERP files

(The monitoring is based on following signals- GPS: LNAV, GAL: FNAV, BDS: CNAV-1, QZSS:LNAV IRNSS:LNAV GLO:LNAV (FDMA))

Time Transfer Through GNSS Pseudorange Measurements: https://e-learning.bipm.org/login/index.php

Allan Tools, https://pypi.org/project/AllanTools/

gLAB GNSS, https://gage.upc.edu/en/learning-materials/software-tools/glab-tool-suite.

Geospatial assessment of impacts of sand mining activities in Zanzibar

Monitoring and managing the impacts of natural resources due to sand mining activities is of utmost importance to ensure their sustainability

Rahma Rashid Amour
Corresponding author, Department of Computer Science and Information Technology, School of Computing, Communications, and Media Studies, State University of Zanzibar, Zanzibar, Tanzania.

Haji Ali Haji
Department of Computer Science and Information Technology, School of Computing, Communications, and Media Studies, State University of Zanzibar, Zanzibar, Tanzania

Abstract

This study assessed the impacts of sand mining activities in Zanzibar by using geospatial technology, focusing on three villages in the North 'B' district of Unguja: Donge-Muwanda, Mchangani, and Misufini. Geospatial technology was employed, utilizing two distinct datasets to analyse the spatial extent of environmental degradation due to sand mining. The first dataset comprised of geographic coordinates of sampled mining sites, acquired through field survey by using the Global Positioning System (GPS). The second dataset involved satellite imagery obtained from the Google Earth application. These datasets were utilized to find the area, volume, and depth of mining sites and create three-dimensional (3D) models for each sand mining site by using ArcMap software and Surfer 19 software. The Google Earth images from 2020, 2021, 2022, and 2023 were utilized to determine changes in vegetation cover before and after the mining activities in the study area. The key finding of the study indicates that there is a high extent of environmental degradation caused by intensive sand mining activities, impacting both the community and environment in surrounding sand mining areas. The study suggests that the results should be used to emphasize the importance of existing policies, guidelines, and laws related to sand mining.

1. Introduction

Sand is a vital natural resource that is commonly found on Earth and is crucial for global economic development [1]. The formation of sand occurs through the process of erosion, where mountain rocks are transported by streams and rivers, resulting in the transportation of sediment that can eventually form sand [2]. The particle size and mineral composition of sand vary, with measurements ranging from 0.06 mm to 2 mm [2]. The availability of sand in certain areas has often led to sand mining activities.

According to Adedeji et al. [3], sand mining is a process that involves the extraction of sand from its natural habitat, which can be carried out in various locations, such as beaches, inland dunes, ocean beds, and riverbeds. This activity has been a source of livelihood for some communities and individuals [1]. Furthermore, sand has numerous applications, including its use in agriculture, as a habitat, in construction, as well as serving as a source of financial gain [4].

Sand mining is a global economic activity that has a significant impact on the economy, society, and environment. Sand mining has both positive and negative social and environmental impacts [5]. The mining process has created employment opportunities and wealth in the mining areas, but it has also resulted in widespread environmental degradation and the erosion of traditional values in society [6]. The mining process has led to the distortion of topography, creation of pools of water for breeding pests, deforestation of areas, and degradation of the ecosystem [6].

Sand mining has emerged as a significant issue globally with far-reaching social, political, economic, and environmental implications. The rapid advancement of science and technology has led to significant changes in the development of urban and rural areas [2]. The increased urbanization and construction of large-scale infrastructure projects have resulted in increased demand for sand resources [7]. It is estimated that between 32 and 50 billion tons of sand are mined globally each year, particularly in developing countries [1].

Tanzania has experienced a rise in public infrastructure investment in recent years, including the construction of roads, bridges, railways, and public buildings. To complete these large projects, sand has emerged as a crucial resource. As a result, there has been a sharp increase in sand mining in Tanzania [8].

Zanzibar Island, as a semi-autonomous part of Tanzania, is seriously affected by sand mining activities due to the increasing sand demand enhanced by rapid urbanization [9]. Sand demand has resulted into the increased number of sand mining sites. Due to inadequate monitoring of sand mining sites and post-management practices, several agricultural lands have been turned into wetlands or borrow pits. Land rehabilitation is required for the sustainability of natural resources and their associated environments [10].

Monitoring and managing the impacts of natural resources due to sand mining activities is of utmost importance to ensure their sustainability. Therefore, it is essential to adopt restoration and conservation measures and employ innovative, improved, and feasible techniques to assess and address these impacts of mining activities. Currently, geospatial techniques have been widely used in investigating the mining or urban environment as they provide a large amount of earth observation data at global, regional, and local scales [11]. Geospatial technology also enables the study of the impacts of mining practices on agricultural environments and suggests environmentally friendly practices [12, 13].

Geospatial technology plays a vital role in the decision-making process of resource utilization by using geographic information systems (GIS). Owing to its capability to handle geographical information, which is crucial for most processes in making decisions, it has significantly impacted the development of decision support systems, especially in the areas of environmental modeling and model development [12].

Numerous researchers have employed geospatial technology to evaluate the impacts of sand mining activities [1, 3, 4, 6, 11]. However, a noteworthy observation showed that the previous studies conducted in Zanzibar have paid limited attention in utilizing geospatial technology to asses the impacts of sand mining [9, 14]. The limited utilization of geospatial technology in Zanzibar may result from a lack of awareness among researchers and policymakers regarding its potential advantages. Furthermore, constrained access to essential tools and resources may act as a barrier to its widespread adoption. The effectiveness of geospatial technology is closely linked to the accessibility and quality of pertinent spatial data.

It is essential to assess the impacts of sand mining activities in Zanzibar using geospatial technology. This technology is potential and allows to acquire data that is referenced to earth easily. The collected data could be used for analysis and visualization of the impacts of sand mining activities, providing a suggestion to minimize social and environmental impacts concerning sand mining activities.

Many tools, including questionnaire and interview, have been adopted in the previous studies conducted in Zanzibar [9, 14], to assess and analyze the impacts of sand mining activities. Though the application of GIS in this study has easily aided in identifying and mapping locations for sand mining within the study area, it also helped to identify consequences associated with sand mining activities.

This study has involved the use of spatial-temporal analysis in examination and interpretation of both spatial and temporal (time-related) patterns and trends of mining areas in North 'B' district in Unguja. This type of analysis explores how phenomena change and interact in both geographical space and over different periods of time. The spatial-temporal analysis involved the use of Google Earth imagery that enabled researchers to leverage its rich dataset, historical imagery, and various tools for visualization. Spatial-temporal analysis in this study involved environmental monitoring that tracked changes in land cover and vegetation from 2020, 2021, 2022, and 2023 around mining areas.

1.1 Study Area

The study was conducted in North 'B'

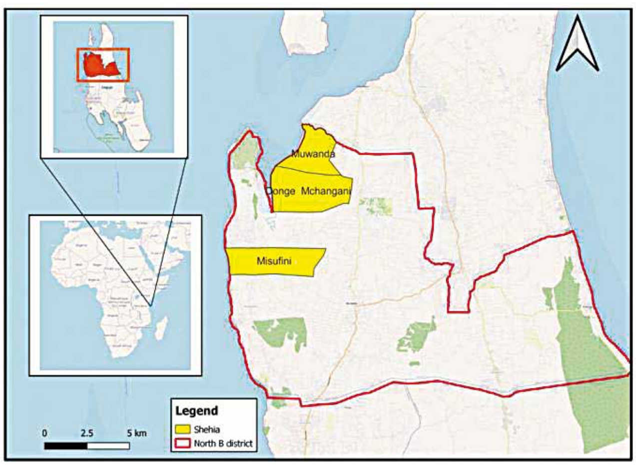

Figure 1. The map shows a location of the study area.
(Source: Open Street Map, 2023)

Unguja Island, Zanzibar, which is 1,666 square kilometers in size. Zanzibar is a semi-autonomous part of the United Republic of Tanzania; it is situated 40 kilometers off the coast of East Africa between latitudes 5° and 6° south and longitudes 39° and 40° east. Unguja covers over 85 kilometers from north to south, and its width varies from 9 kilometers in the north to nearly 35 kilometers in the south [15].

The study area was North 'B' District, which is located in the Northern Region of Unguja Island. This region is divided into two administrative districts, North ‘A’ and North ‘B’, both of which fall under the purview of the Local Governance in Zanzibar Legislative Regulation [16]. The North ‘B’ District covers an area of approximately 234 square kilometers. Figure 1 shows the location of the study area on a map of Unguja Island.

According to the Population and Housing Census of Tanzania of 2022, the total population of Zanzibar was 1,889,773 people, with a yearly growth rate of 3.7%. However, the population in the North Region of Unguja is approximately 257,290 people. The North 'B' District has a current population of 81,675 people, accounting for 6.2% of the total population of Zanzibar.

Zanzibar Island’s maximum temperature ranges from 28°C to 33°C per year. In the meantime, the low annual temperature ranges between 22°C to 25°C. High temperatures and heavy rainfall are two of Zanzibar's defining characteristics throughout the year [18]. It is important to note that the short rainy season occurs in either September or October, while the long rainy season spans from March to May.

2. Methodology

This study was conducted in the North 'B' district of Unguja Island, focusing on sand mining sites. The researchers selected villages based on the proximity of sand mining activities. The study was conducted in areas that are severely impacted by sand mining. The afflicted areas were chosen by using purposeful sampling because they meet the researchers’ objectives. The study used primary and secondary data. The primary data was geographic coordinate and secondary data used was Google Earth imagery. For acquiring secondary data, convenience sampling was used to get the satellite data from the portal.

The study used current and past Google Earth imagery to find the spatial extent of environmental degradation as a result of sand mining activities in the North ‘B’ district. The researchers selected three (3) Shehias out of 31 Shehia in North ‘B’ for analyzing the impacts of sand mining, where sand mining is commonly carried out. The Shehias selected were Donge-Muwanda, Donge-Mchangani, and Misufini. One mining site significantly impacted by sand mining activities was chosen from each Shehia. In these areas, satellite imagery was obtained between the year 2020 to 2023. Though, prior to 2020, these areas exhibited no mining operations; instead, they were characterized by vegetation and trees.

The geographic coordinates of these mining sites were acquired through on-site surveys employing a GPS. For precise identification of sampled mined areas, approximately two random geographic coordinate points were documented at each site. The GPS tool used was Garmin GPSMAP 64sx. This handheld GPS device was used for the study due to its user-friendly features, higher reliability and accuracy. Garmin GPS devices offer real-time tracking capabilities and play a crucial role in enhancing the efficiency and effectiveness of spatial data collection and analysis. The coordinates obtained were later fed into the Google Earth desktop application software for precise identification of each of the mining sites in the satellite imagery (ground truthing).

After precise identification of mining site in Google Earth application, the ‘add path’ tool was used to generate coordinates points in the mined area. The researchers created many random points to ensure the mined area is covered. The rationale for generating many coordinate points was to facilitate a smooth surface. In simple terms, the higher the number of random points created, the smoother the surface. The random points generated saved in the computer database with the “kml” file format. The saved files of random points of three mining sites were then fed into the TCX Converter tool to generate the elevation value of each point and change the file extension from KML to CSV format. The TCX Converter tool is commonly used for converting GPS-related data formats. In this study, this tool helped to enhance compatibility between Google Earth, Surfer 19 software and ArcGIS software by ensuring the data are in suitable format for integration and analysis.

The (x, y) coordinates and elevation database of all the sample mining sites created were exported to Surfer 19 Software, where they were converted to a grid using Inverse Distance to a Power gridding method. The 3D surface analyses were carried out using gridding values and 3D surface mapping tools. Minimum and maximum elevation values were obtained from Surfer 19 during analysis. This method of creating 3D mapping has also been implemented by Oluku and Asikhia [6] for easy visualization of the extent of degradation in the mined area.

Moreover, Google Earth application was used to generate the (x, y) coordinates points that were used to create polygon. The polygon used to find the values of area and volume of mined sand. The saved boundary values of three mined areas were then loaded into ArcMap 10.7. Initially, the coordinate points were converted from point to the path, then the path to the polygon. Furthermore, the ArcMap software was used to calculate the area of a polygon using the "Calculate Geometry" tool. In the "Calculate Geometry" dialog box, the "Area" field was selected as the property to calculate the area. This methodology helped the researchers to calculate and populate the value of area of each polygon.

Additionally, in calculating the volume of mined sand, similar procedures were adopted as in earlier steps in ArcMap 10.7. After adding a new field named 'Volume,' the 'Field Calculator' was selected by right-clicking on the new field in the attribute table. In the Field Calculator dialog, authors constructed an expression to calculate volume. The formula used for finding volume (V) was given by the product of area (A) and depth (D).

After setting up the expression, ArcMap automatically computed the volume of sand excavated at each mining area.

The difference between the maximum and minimum pixel' elevation is referred to as the "depth" of the mining area. The results obtained, which were values of depth, area and volume of sand mined, were considered in assessing the spatial extent of environmental degradation as a result of sand mining activities in the North 'B' district. Figure 2 demonstrates the flow-diagram of the methodology employed in the present study.

3. Results and Discussion

The study findings show that the environmental degradation in the North 'B' district is more significant due to daily and yearly increases in sand mining activities. Figure 3 shows the activities of sand miners which contribute to land degradation in the area of Donge-Mchangani.

The organization of the results in this section is based on Google Earth imagery and 3D images of mined areas. The 3D images show the current situation of the mining areas and reveal the extent of land degradation. The Google Earth images depict the condition of the mined area before as well as after the end of mining operations. Additionally, Table 1 shows the spatial measurement of extent of environmental degradation of the mined area. These measurements were obtained by analyzing the Google Earth Images collected in the year 2023.

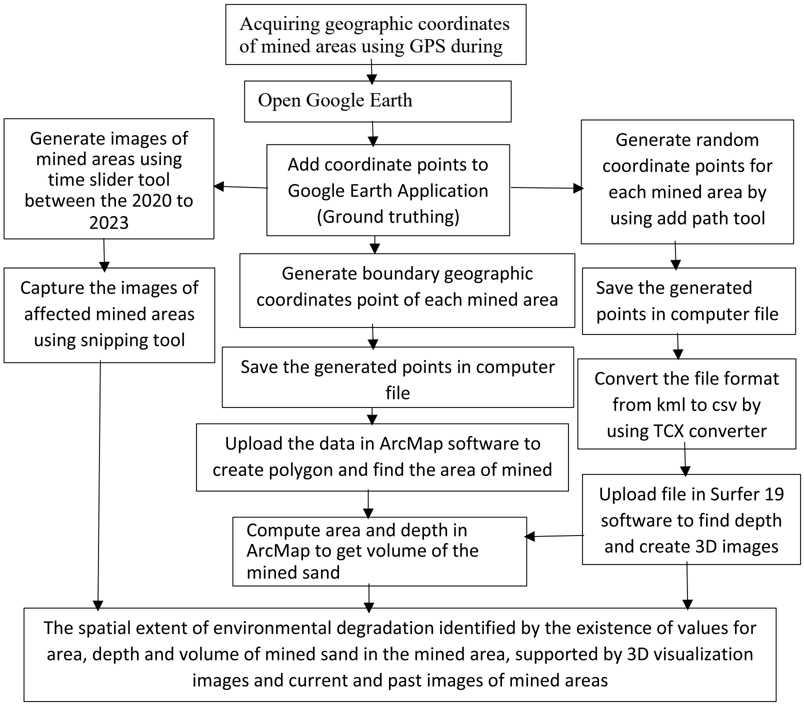

Figure 2. Methodology employed in the study.

Figure 3. Activities of Sand Miners Showing the Extent of Land Degradation.

Table 1. GIS/Spatial Measurements of Mined Areas.

Mined Area	Coordinates		Elevation (m)		Approx. Area(m^2)	Depth (m)	Volume (m^3)
	Latitude	Longitude	Min	Max			
Donge-Mchangani	5°55'57.23"S	39°13'59.39"E	10	21	79,380	11	873,180
Donge-Muwanda	5°54'21.34"S	39°13'55.11"E	8	19.5	45,867	11.5	254,561.8
Misufini	5°58'37.79"S	39°12'23.67"E	13.5	21	27,411	7.5	205,582.5

From Table 1, the results show that, the elevation of the mined area at Donge-Mchangani was 11 m above the sea, covering an area of 79,380 m2 and the volume of sand excavated was 873,180 m3. On the other hand, at Donge-

Figure 4a. Satellite Imagery. *(Source: Google Earth, 2023)*

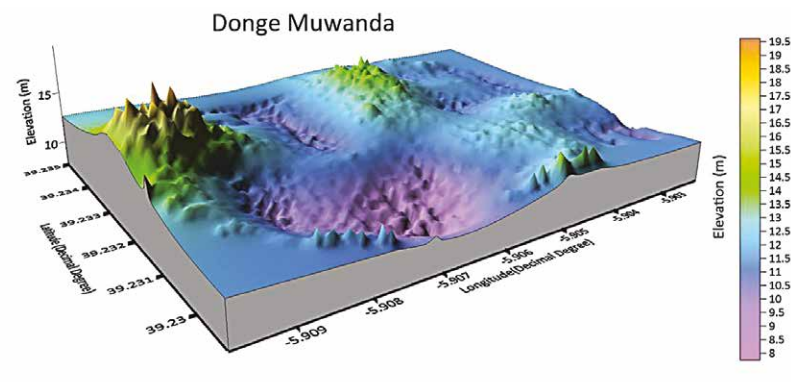

Figure 4b. 3D Image.

Muwanda the elevation was 11.5 m with an area of 45, 867 m2 and 254,561.8 m3 is the volume of sand that had been excavated. In Misufini, the elevation is 7.5 m, covering an area of 27,411 m2, and 205,582.5 m3 is the volume of sand that had been excavated from the area.

Figure 4, Figure 5, and Figure 6 show the spatial extent of environmental degradation causes by sand mining activities in the area of Donge-Muwanda, Donge Mchangani and Misufini respectively. They also show the depth of degraded land. Figure 4a and Figure 4b show the Google Earth imagery and 3D image of Donge-Muwanda, respectively. The results show that the spatial extent of environmental degradation in this area is very high. During 2020, the area was covered with vegetation, and villagers used this area for agricultural activities. In the year 2021, the area was also covered with vegetation. However, in the year 2022 and 2023, the results show that the area is degraded since the top layer has been removed due to sand mining activities that made the bare land. The results show that the land is no longer useful for agricultural purposes due to the extensive degradation.

Figure 5a and Figure 5b show the Google Earth imagery and 3D image of Donge-Mchangani, respectively. During 2020 and 2021, this area was covered with trees. However, in the year 2022, mining activities were carried out and continued to the year 2023, resulting a degraded land. The results show that mining activities in this area have caused deforestation and damaged the ecosystem. Before mining started, there was a road crossing the area, but when mining activities started, the local road was not spared from destruction either.

Figures 6a and 6b depict the Google Earth imagery and 3D representation of the Misufini area, respectively. In 2020, the area was densely vegetated with trees. However, mining activities in 2021 led to extensive deforestation, leaving the terrain strewn with tree roots. Additionally, during the same year, the imagery indicates water accumulation on the left side of the area, impacting local fauna, flora, and human inhabitants. Despite these changes, the environmental degradation in the area was relatively limited, as the mining pit's depth was shallow. Typically, deeper mining operations result in greater loss of fertile soil. Presently, the area is no longer operational and shows signs of natural recovery, characterized by the emergence of small bushes and grasses, which is a positive indication of ecological restoration.

The findings of the study indicate that the impact of sand mining on both the environment and local communities is inevitable, particularly due to the close proximity of mining sites to residential areas. The resulting environmental repercussions are significant, affecting both the natural surroundings and social dynamics. Furthermore, the outcomes derived from this research are transferable to similar regions across Unguja and Pemba Islands, given the comparable environmental characteristics and lifestyle patterns prevalent in these areas.

Land degradation resulting from sand mining activities exerts a detrimental effect on both the environment and nearby communities. Through the examination of current and historical satellite imagery in mining areas, this study has found substantial land degradation caused by sand mining operations. This corroborates the findings of previous studies [3, 4, 6], which similarly highlighted the adverse environmental effects of sand mining activities.

Oluku and Asikhia [6] employed geospatial technology to analyze the spatial extent of environmental degradation, a methodology closely aligned with the approach undertaken in this study. Despite minor variances in methodology, such as the utilization of DEM data by Oluku and Asikhia

[6] versus satellite imagery in this study, both investigations sought to delineate and visualize the extent of land degradation. The methodology proposed in this study has been shown to be useful for detecting forest disturbance, degradation, and environmental damage.

Similarly, Odeyemi and Atejioye [4] analysed the impacts of sand mining by using GIS technology. Their study's findings aligned with the findings of this study, since sand mining is the source of land degradation in mining areas. Land degradation was measured by three parameters including the depth, volume, and areas of the mined pits. However, the methodology adopted in their study was different compared with the one used in this study. Odeyemi and Atejioye [4] used Triangulated Irregular Network (TIN) analysis to find the volume of mined sand. This study used the Field Calculator tool to compute the parameter of depth and area that resulted in the parameter of the volume of sand that has been extracted. Both methods involved the use of ArcGIS software in the analysis.

Furthermore, the findings of the present study were obtained by analyzing the Google Earth Data. These data are very significant for assessing the impacts of sand mining activities, investigating and identifying sand mining areas for sustainable development, and environmental monitoring. Prasad et al. [11] has also used this technology in mapping and analyzing sand mining activities.

Moreover, the present study found that sand mining has caused serious environmental problems, including land degradation, in mining areas. The study by Adedeji et al. [3] show the impacts of sand mining on the environment, which include water quantity, and air pollution, which are also found in this study. Both studies used GIS technology to assess the impacts of sand mining activities.

The findings of this study also revealed that villagers have lost their farmland and vegetation due to massive environmental degradation caused by sand mining activities. This finding looks similar to what was said by previous scholars [9, 16, 17], who mentioned that sand mining has caused the removal of vegetation and destruction of the soil's top layer. They also claimed that sand mining has been alleged to result in the degradation and decline of farmland as well as agricultural productivity.

Furthermore, the findings of this study show that sand mining has resulted a deforestation and damage the ecosystem. This finding also align to the results mentioned by precious scholars [7, 13], who noted that deforestation is primarily caused by sand mining activities in mining areas. Additionally, the findings of this study indicated that deforestation has negative effects on animals, plants and people living near mining areas.

With regard to the findings, this study aimed to provide the following contributions: firstly, to enhance the public's awareness of the current impacts associated with sand mining activities in the North 'B' district of Unguja. Secondly, the study aimed to contribute knowledge on the methods and tools used to assess the impacts of sand mining. Our study faced methodological limitations due to the use of Google Earth imagery from 2020, 2021, 2022, and 2023. The imagery was used to analyze mining areas and assess the impacts associated with sand mining activities. Another limiting issue was the time-limit for data collection. The researchers required to collect coordinate points from the affected areas. These data were used for ground truthing. However, mining sites are in dangerous bushy areas and very far from towns, thus researchers had to wait to be accompanied by government officials when they were

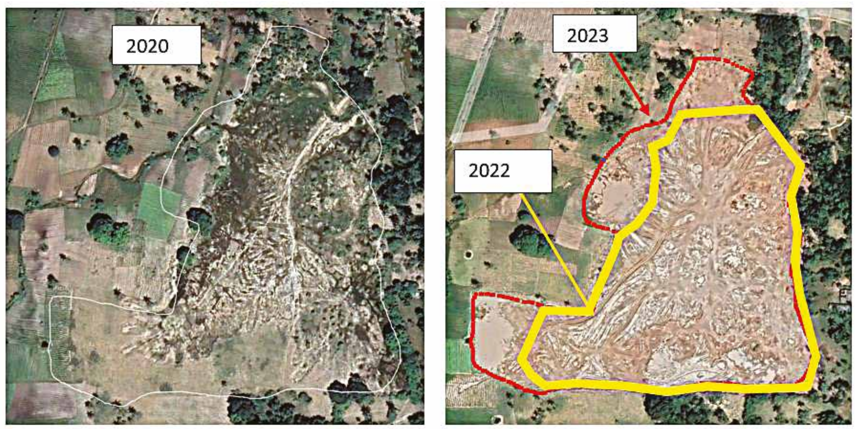

Figure 5a. Satellite Image. *(Source: Google Earth, 2023)*

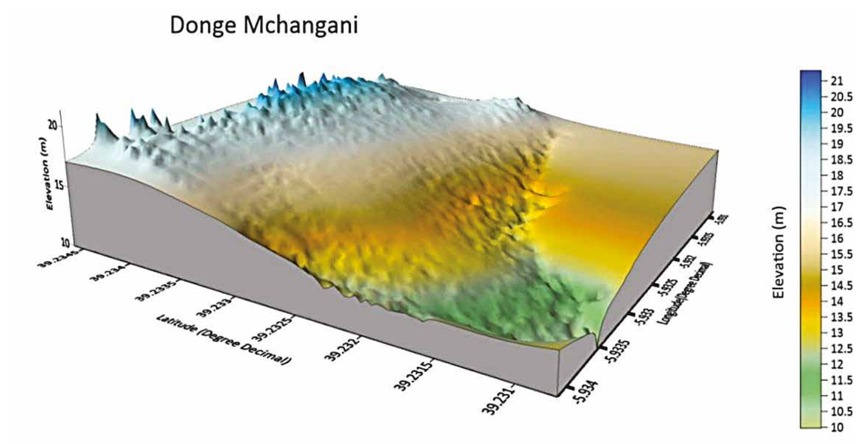

Figure 5b. 3D Image of donge-Mchangani.

Figure 6a. Satellite Image. *(Source: Google Earth, 2023)*

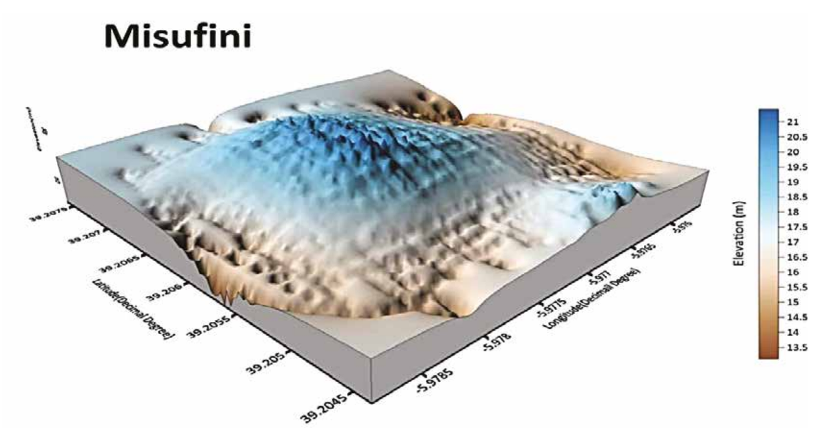

Figure 6b. 3D Image of donge-Misufini.

free from their other commitments. This has led the researchers to spend much time in the process of data collection. Additionally, due to time constraints, the study was also limited to use only three Shehias out of thirty-one Shehias, and only one mining site from each Shehia.

4. Conclusion and Recommendation

This study investigated the impacts of sand mining activities in Zanzibar by using geospatial technology. The study was conducted in Zanzibar, specifically in the North 'B' district located in the Unguja Islands, which is where the majority of sand mining activities take place.

The study has demonstrated that sand mining activities have negative effects on the environment and local communities living near the mining areas. Based on the results, the study shows that sand mining has caused massive effects, including land degradation, deforestation, loss of vegetation, loss of farmland, and general damage to the ecosystems.

This study suggests that the results should be utilized to underscore the importance of current policies, guidelines, and laws related to sand mining. For example, in August 2022, an Expression of Interest (EOI) was lodged to formulate the Zanzibar Mining Policy, Guidelines, and Laws. This was aimed to promote sustainable management and minimize the overuse of sand resources that can results environmental degradation.

Moreover, the study suggests that the Government of Zanzibar should commence a high-level decision-making session if one does not already exist, with participation from all stakeholders to discuss the issue of sand mining. The objective is to collaboratively address the negative impacts of sand mining activities and formulate prompt solutions. This should be done through the appropriate Ministry and Department of Minerals since the villagers in the North ‘B’ district are at high risk of losing their life and farmland due to continuing sand mining activities.

Additionally, the study recommends that the Department of mines and Minerals in Zanzibar use public media, including television, radio, newspapers, and social media to provide knowledge of effects of sand mining. This approach aims to raise awareness among community members, especially miners, about the environmental degradation caused by ongoing sand mining activities. The Department should also enforce the miners to invest in and repair the degraded mined areas, to minimize the possibility risk of landslides and accidents. The community members should play a crucial role in minimizing environmental degradation. This can be achieved by adopting various sustainable practices and actively participating in conservation efforts, such as involvement in tree-planting initiatives to enhance green spaces and combat deforestation. Additionally, staying informed about environmental issues and solutions through educational programs and workshops is essential.

This study involved the use of Geospatial Technology to assess sand mining impacts. However, there is a large knowledge gap in assessing more impacts of sand mining activities, which include rise in land surface temperature and loose of vegetation and farms. These impacts also identified by previous researches [3, 4]. There are many reasons besides sand mining that lead to rising in land surface temperature and loss of vegetation and farmland, including urbanization. Therefore, further research is needed to find out the contribution of sand mining activities to the rise of land surface temperature, and the contribution of sand mining activities in the loss of vegetation and farm land. Further research could also be done to determine the significance of sand mining activities to the national economic development of developing nations like Tanzania at large

Additionally, the future perspective of study is to apply a Machine Learning or Artificial Intelligence to monitor and predict the current and the future condition of degraded land, using historical data.

Contributions of Co-Authors

Rahma Rashid Amour

Developed the concept, carried out data collection, performed data analysis, and compiled the paper.

Haji Ali Haji

Reviewed the paper and provided technical support on procedures and resources

References

[1] Nwobodo TN., Ogbuene BE., Nzeadibe TC., *Effects of sand mining on land use/land cover on river environment in developing countries: a case study of ava river in Enugu state, Nigeria*, Ikenga, **22**(3): p.1–25, 2021.

[2] Rukmana D., Salman D., Alimuddin I., Arsyad. *Economic and environmental impacts of sand mining activities at Sadang river Pinrang Regency, South Sulawesi*, IOP Conf Ser Earth Environ Sci., **575**(1): p. 012043, 2020.

[3] Adedeji OH., Adebayo HO., Sotayo EI., *Assessing environmental impacts of inland sand mining in parts of Ogun State, Nigeria*, Ethiopian Journal of Environmental Studies and Management, **7**(5): p. 478–487, 2014.

[4] Odeyemi C., Atejioye A., *Analysing impact of sand mining in Ekiti State,* World J Res Rev, **6**(2): p. 26–31, 2018;

[5] Mngeni A., Musampa CM., Nakin MDV., The *effects of sand mining on rural communities,* Sustain Dev Plan VIII, **210**: p. 443–453, 2017.

[6] Oluku S., Asikhia MO., *Geospatial assessment of the impacts of sand mining activities in Benin City, Edo State Nigeria,* J Geogr Environ Earth Sci Int., **25**(1): p. 46–57, 2021.

[7] Koehnken L., *Impacts of sand mining on ecosystem structure*, process & biodiversity in rivers, 2018. link: https://d2ouvy59p0dg6k.cloudfront.net/downloads/sand_mining_impacts_on_world_rivers__final_.pdf.

[8] Christina S., Suykens B., *River Sand commodity chains in Tanzania*, 2022. Link: www.gicnetwork.be.

[9] Ladlow C., *An assessment of the impact of sand mining: Unguja, Zanzibar*, ISP Collection, p 1–41, 2015.

[10] Abraham CM., Essien K., Umoh EU., Umoh EC., Ehiremem LE., et al., *Towards effective monitoring of sand mining sites and post management techniques in sand dredged environment of Akwa Ibom State, Nigeria*, Glob J Ecol., **6**(1): p. 092–099, 2021.

[11] Prasad M., Reddy MR., Sunitha V., *Mapping of River Sand Mining Zones Using Remote Sensing and GIS: A Case Study in Parts of Papagni and Pennar River Beds, YSR district Andhra Pradesh*, Asian Academic Research Journal of Multidisciplinary, **3**(7): p. 45–55, 2016.

[12] Prasad, M., Reddy, YS., Balaji, E., Sunitha, V., Ramakrishna, MR., *Application of geospatial technology in evaluating the impact of mining associated urbanization on agricultural lands*, Nat. Environ. Pollut. Technol., **18**(3): p. 1041–1044, 2019.

[13] Ahmad, F., Prasad, RC., Goparaju L., *Geospatial technology perspectives for mining vis-a-vis sustainable forest ecosystems*. Present Environ Sustain Dev., **11**(1): p. 219–238, 2017.

[14] Mohammed Z., *Sand mining management systems and their effects on social and environmental aspects in Unguja, Zanzibar*, Int J Sci Environ Technol., **9**(6): p. 885–888, 2020.

[15] FAO, Evaluation of land resources in Zanzibar: phase 1 & 2, 1990. link: https://www.fao.org/4/as019e/as019e.pdf.

[16] Tidemand, Mukandala, Makaramba, Othman, *Local governance in Zanzibar*, UNDP report, 2003. link: https://www.dege.biz/Zanzibar.pdf.

[17] Jaeger W., *The hidden costs of relocating sand and gravel mines*, Resources policy, **31**(3): p.146–164, 2006.

[18] Pitchaiah S., *Impacts of sand mining on environment-a review*, International Journal of Geoinformatics and Geological Science, 4(1): p. 1–5, 2017.

Originally published in Journal of ICT Systems, Volume 2(1) Pages 59-71, 30 June 2024. Republished with authors' permission.

UAE, Bahrain boost space and climate monitoring with satellite launches

The UAE and Bahrain successfully launched their satellites, Etihad-SAT and Al-Munther, to enhance environmental monitoring and advance scientific research.

The Etihad-SAT, developed by the Mohammed Bin Rashid Space Centre (MBRSC), was deployed from Vandenberg Air Force Base in California aboard SpaceX's Falcon 9 rocket.

The radar-equipped satellite can capture high-precision images in all weather conditions and monitor various environmental factors, including detecting oil leaks, tracking maritime traffic, and supporting agricultural initiatives. This satellite launch is part of UAE's expanding space program, which began with the formation of the UAE Space Agency in 2014 and includes the Hope Probe mission to Mars.

Bahrain also successfully launched their own version, Al-Munther, the first domestically designed and developed satellite, also aboard the same Falcon 9 rocket. *www.newarab.com*

New research centre At IIT Madras

Indian Space Research Organisation (ISRO) chairman V Narayanan inaugurated a new research centre of thermal sciences for space applications at the Indian Institute of Technology Madras (IIT Madras).

This state-of-the-art research facility, housed at the Department of Mechanical Engineering, will focus on critical advancements in spacecraft and launch vehicle thermal management, a key area for India's expanding space ambitions. This apart, the centre will also serve as a nodal centre for research in heat transfer, cooling systems and fluid dynamics. These are essential for the next generation of spacecraft and satellite technologies. Scientists and engineers from ISRO will work alongside faculty and researchers from IIT Madras to address complex thermal challenges in space applications. *www.etvbharat.com*

Chandrayaan-5 Mission Approved

The government of India has approved the Chandrayaan 5 mission, and it will carry a whopping 250 kg rover to the lunar surface, according to the Indian Space Research Organization (ISRO) Chairman V Narayanan.

It will be the fifth flight as part of the Chandrayaan programme, also known as the Indian Lunar Exploration Programme, and aims for the exploration of the Moon.

The Chandrayaan-3 was a resounding success making India the first country in the world to make a soft landing on the South Pole of the Moon. India also became the fourth nation after the erstwhile USSR (now Russia), the US, and China to make a soft landing on the Moon.

While Chandrayaan-3 carried a 25-kg rover named 'Prayagyaan,' the new Chandrayaan-5 mission, in collaboration with Japan, will feature a much heavier 250-kg rover. *www.ndtv.com*

AI Capabilities to Turn Geospatial Satellite Imagery into Actionable Insights

Planet Labs recently announced that it will begin using Anthropic's Claude's Large Language Models (LLMs), to revolutionize how we understand and analyze our changing planet. This collaboration will combine Planet's deep stack of daily geospatial data with Claude's advanced AI capabilities to analyze complex visual information at scale and uncover insights about our changing planet.

China adds to SuperView remote sensing constellation

China recently added to a commercial high-resolution remote sensing constellation with the launch of a pair of SuperView Neo-1 satellites. The China Aerospace Science and Technology Corporation (CASC) announced launch a success within an hour of liftoff.

The satellites are part of the "China Siwei New Generation Commercial Remote Sensing Satellite System," which now has nine satellites in orbit and will grow to a total of 28 spacecraft. CASC describes the satellites as currently having the highest spatial resolution of commercial remote sensing satellites within China. The SuperView constellation currently consists of four Neo-1 optical satellites, four Neo-2 SAR satellites, and one Neo-3 ultra-large width satellite. SAR enables all-weather imaging while optical satellites provide high-resolution detail.

Shiv Nadar University Signs MoU with NRSC

Shiv Nadar University has signed a Memorandum of Understanding (MoU) with the National Remote Sensing Centre (NRSC), a branch of the Indian Space Research Organisation (ISRO), to accelerate research in space technology and artificial intelligence (AI). The association will contribute to research on imagery from satellite applications for ecological and urban development, disaster management using satellite photography and forecasting analytics, AI-driven precision farming for crop monitoring and yield optimization, climate resilience studies that use observational data, and autonomous UAV-based environmental assessments.

Saudi Arabia, Korea Sign MoU

The Saudi Space Agency (SSA) has signed a MoU with the Korea AeroSpace Administration (KASA) to enhance cooperation in the space sector. The MoU aims to support and strengthen the strategic partnership between the two entities by establishing a framework for implementing collaborative activities and programs in space-related fields. These include deep space technologies, manned spaceflight programs, satellite launches and payloads, space science and engineering capacity-building, and the exchange of knowledge and expertise in advanced space applications. *my.gov.sa*

FORM IV

Place of publication:	New Delhi	Publisher's name:	Sanjay Malaviya
Periodicity:	Monthly	Nationality:	Indian
Printer's name:	Thomson Press	Address:	499D, Shipra Sun City, Indirapuram, Gaziabad
Nationality:	Indian	Editor's name:	Bal Krishna
Address:	Mathura Road, Faridabad, India	Nationality:	Indian
		Address:	A 002, Mansara Apartments, C 9, Vasundhara Enclave, Delhi – 110096

I, Sanjay Malaviya, hereby declare that the particulars given above are true to the best of my knowledge and belief.

March 1, 2025 Signature of publisher

SDB solution for nautical charts in shallow waters

TCarta has introduced a new line of Satellite Reconnaissance Charts designed to complement official marine navigation maps in shallow waters. These digital maps, derived from recently acquired satellite imagery, adhere to International Hydrographic Organization S-57 and S-100 data model standards, mirroring the appearance and symbology of official navigation aids. The new products are particularly valuable for shallow water navigation, where official nautical map products, primarily designed for commercial shipping lanes, may lack detail. *tcarta.com*

China unveils first homegrown space mining robot

China's first space mining robot has been developed by the China University of Mining and Technology (CUMT). It not only adapts to the microgravity conditions of space but also navigates the rugged, cratered terrain of asteroids. The prototype has now filed patents with relevant authorities and successfully cleared preliminary reviews, the report said.

Space mining robots are confronted with geological exploration and mineral collection on extra-terrestrial bodies, requiring essential drilling capabilities. Under Earth's gravity, the robot's own weight is sufficient to support the drill's penetration. However, lunar gravity is only one-sixth of Earth's, and asteroids often exhibit ultra-low gravity, posing significant challenges for drilling into their surfaces.

To address the problem caused by microgravity, inspirations were drawn from insect claw-and-spine structures, and equipped the robot with specialized clawed limbs. Its array-style claw design enhances adhesion and anchoring capabilities in microgravity, allowing the robot to stabilize itself for sampling while adapting its movement to terrain. *www.globaltimes.cn*

ESA and EnSilica partnership for resilient GNSS

In partnership with the European Space Agency (ESA), EnSilica will design and develop a key silicon component to enable next-generation resilient multi-band GNSS capabilities. These are vital to ensuring the world's critical infrastructure and services remain robust and secure in the face of evolving global threats.

The ESA, NAVISP Element 2 programme helps to increase the competitiveness of participating European states in the global market for satellite navigation and enables these countries to be well positioned to capitalise on emerging market opportunities across Positioning, Navigation and Timing ("PNT") technologies and services.

EnSilica is working with support from ESA and UKSA, with the latter organisation awarding the Company £10.38 million in February 2025 for a development project under its Connectivity in Low Earth Orbit programme. *www.ensilica.com*

NASA lunar experiment establishes first GPS signal on the Moon

NASA and the Italian Space Agency made history on March 3 when the Lunar GNSS Receiver Experiment (LuGRE) became the first technology demonstration to acquire and track Earth-based navigation signals on the Moon's surface.

The LuGRE payload's success in lunar orbit and on the surface indicates that signals from the GNSS (Global Navigation Satellite System) can be received and tracked at the Moon. These results mean NASA's Artemis missions, or other exploration missions, could benefit from these signals to accurately and autonomously determine their position, velocity, and time.

The road to the historic milestone began on March 2 when the Firefly Aerospace's Blue Ghostlunar lander touched down on the Moon and delivered LuGRE, one of 10 NASA payloads intended to advance lunar science. Soon after landing, LuGRE payload operators at NASA's Goddard Space Flight Center in Greenbelt, Maryland, began conducting their first science operation on the lunar surface.

The mission will operate for 14 days providing NASA and the Italian Space Agency the opportunity to collect data in a near-continuous mode, leading to additional GNSS milestones. LuGRE is the first Italian Space Agency developed hardware on the Moon, a milestone for the organization. *www.nasa.gov*

ESA to develop optical technology for navigation

The European Space Agency (ESA) has signed a contract with a consortium of European companies to conduct a definition study (Phase A/B1) and associated critical technology predevelopment to drive the development of optical PNT technology.

This initiative marks the initial phase toward a potential in-orbit demonstrator for optical time synchronization and ranging, which is scheduled for proposal at the ESA Council at the Ministerial Level in November. According to ESA, the primary objective is to validate inter-satellite optical links for future implementation in operational satellite navigation systems.

Optical technology presents promising advancements in navigation accuracy and robustness. While optical links, which use laser beams for data transmission, are already established in satellite communications, their application in navigation requires further technological development and in-orbit validation.

The consortium, led by German OHB System, comprises 33 companies from various ESA member states. Following the initial study, the next phase would involve developing and testing the technology in orbit to validate novel system concepts and explore new architectures. The results will assess the readiness of optical technology and inform decision-makers about its potential incorporation into future operational systems.

Laser-based technology offers the potential for enhanced system resilience and robustness, potentially reducing dependence on space atomic clocks and ground segments. Optical links also provide natural immunity to jamming and spoofing attempts.

The high data transfer rates of inter-satellite optical links could enable new, more robust architectures, supporting a multi-layer system approach to navigation. This aligns with the vision of ESA's low-Earth orbit (LEO)-PNT program.

Additionally, optical systems can significantly improve the performance of current navigation systems. Experts anticipate achieving millimeter-level spatial accuracy and picosecond-level timing, which could ultimately lead to enhanced services benefiting billions of users worldwide.*www.esa.int*

AFRL contract to Xona to demo LEO GPS alternative

The Air Force Research Laboratory awarded Xona Space Systems a contract to demonstrate and refine its commercial PNT solutions for Department of Defense (DOD) missions. The agreement, facilitated through the Space Technology Advanced Research — Fast-tracking Innovative Software and Hardware (STAR-FISH) program, increases Xona's total contracted commitments to more than $20 million.

Under the contract, Xona will evaluate its PULSAR satellite navigation service across commercial user devices in scenarios where GPS/GNSS signals may be denied or challenged. Testing will focus on assessing resistance to jamming and spoofing, reducing multipath interference and implementing secure key distribution protocols. The initiative aims to expedite the development of advanced alternative PNT capabilities in commercial off-the-shelf equipment, aligning with DOD requirements for rapid deployment.

Xona has collaborated with GPS/GNSS hardware providers QinetiQ, StarNav and Locus Lock to integrate PULSAR-enabled devices. These partners will participate in performance demonstrations as part of the multi-year effort, which includes leveraging simulation tools and plans to utilize the first PULSAR satellite scheduled for launch in June 2025. *www.xonaspace.com*

R-EGI proves resilient navigation in GPS-denied flight tests

The Air Force Life Cycle Management Center (AFLCMC) PNT Program Office and Integrated Solutions for Systems (IS4S), in collaboration with AEVEX Aerospace, has announced the successful completion of Alternative Positioning, Navigation, and Timing (PNT) flight tests for the Resilient-Embedded GPS/INS (R-EGI) Modular Open Systems Architecture (MOSA). This achievement marks a monumental step forward in the development of R-EGI, demonstrating its ability to integrate a "plug & play" third-party alternative PNT capability that ensures reliable navigation in GPS-denied environments.

The R-EGI system's open MOSA design enables seamless integration of government and third-party applications to address emerging navigation threats. Its Mission Capability Navigation (MCNAV) component allows for seamless integration of external alternative PNT solutions under challenging conditions.

During six test flights on a Special Operations Command C-146A Cougar aircraft, R-EGI operated successfully in GPS-denied environments, validating the system's resilience and capacity for real-time adaptability. *mar.com@is4s.com*

Astranis advances resilient GPS technology for US Space Force

Astranis has completed a critical demonstration for the U.S. Space Force's Resilient GPS (R-GPS) program, showcasing its ability to transmit core GPS waveforms using software-defined radio hardware. Conducted ahead of schedule and within budget, the demonstration highlights Astranis' ability to adapt its flight-heritage high-orbit satellite hardware to meet new resilience requirements for the Space Force.

The test took place at Astranis' headquarters in San Francisco, California, using a flight-like software-defined radio and positioning, navigation and timing algorithms provided by Xona Space Systems, a partner and subcontractor for the R-GPS program. Astranis transmitted a GPS Course Acquisition (C/A) navigation signal through its resilient GPS payload and demonstrated signal acquisition and recovery of Legacy Navigation messages with an off-the-shelf GPS receiver. This validated that its resilient GPS design, Nexus, complies with GPS specifications "out of the box," ensuring compatibility with existing user equipment without requiring costly upgrades. *www.astranis.com*

FAA and NAWCAD advance CRPA approval process

The Federal Aviation Administration (FAA) has partnered with the Naval Air Warfare Center Aircraft Division (NAWCAD) to initiate steps toward approving Controlled Reception Pattern Antennas (CPRAs) for use in aircraft. This collaboration addresses GPS/GNSS jamming and spoofing threats, with the current focus on a Request for Information (RFI) to study anti-jamming and anti-spoofing technologies. The RFI, published on SAM.gov, aims to identify and evaluate vendors' antenna technologies for potential integration into civilian aircraft.

CPRAs could significantly mitigate terrestrial-based GPS/GNSS jamming and spoofing, enhancing aviation safety by preserving situational awareness and reducing pilot workload during disruptions. The technology's effectiveness in neutralizing ground-based threats positions it as a critical tool for maintaining reliable navigation systems. *rntfnd.org*

Eos Positioning Systems redesigns Eos Tools Pro on iOS

Eos Positioning Systems has launched a redesigned Eos Tools Pro app on iOS. The redesigned app includes a reorganized settings menu to improve the organization of all configuration options, offering a centralized space for users to manage their GNSS preferences and optimize workflows. The new interface has been revamped to take advantage of Split View mode on iPadOS to view all pertinent information when using Eos Tools Pro in conjunction with a data-collection app. This is particularly useful for Skadi Tilt Compensation and Skadi Smart Handle users. *eos-gnss.com*

SatNav receiver by STMicroelectronics

STMicroelectronics has unveiled the Teseo VI family of GNSS receivers. The new receivers integrate multi-constellation and quad-band signal processing on a single chip, achieving centimeter-level accuracy for various applications.

The Teseo VI family includes the STA8600A and STA8610A models, featuring dual independent Arm Cortex-M7 processing cores. The Teseo VI+ variant can host enhanced positioning engines developed by third-party companies, providing real-time kinematics for centimeter position accuracy. The Teseo APP2 STA9200MA operates dual cores in lockstep, offering hardware redundancy for applications requiring ISO 26262 ASIL-B functional safety compliance12. *newsroom.st.com*

Quectel unveils LG580P GNSS RTK module

Quectel Wireless Solutions has launched LG580P, a multi-constellation, multi-band GNSS module designed for high-precision positioning. The module supports multi-band signals across L1, L2, L5, and L6, enabling real-time kinematic (RTK) positioning and integrating a dual antenna heading algorithm for enhanced accuracy and reliability. *quectel.com*

SBG Systems expands GNSS receiver options

SBG Systems has upgraded its inertial navigation systems — Ekinox, Apogee and Navsight— with new GNSS receiver options designed to offer greater flexibility while maintaining high precision and reliability.

The latest update introduces three additional GNSS receiver variants, each tailored to specific regional and application needs. These include:

- **Marinestar:** This variant supports Fugro Marinestar, delivering precise point positioning (PPP) with cm-level accuracy via L-band corrections without requiring a base station. It is optimized for marine applications such as hydrographic surveys and dredging.
- **HAS Ready / NavIC:** Designed for future compatibility, this variant includes Galileo E6 support for the upcoming Galileo High Accuracy Service (HAS), offering free decimeter-level PPP corrections globally. Additionally, it supports the Indian NavIC system, making it suitable for applications in urban environments, aviation and operations in India.
- **Centimeter-Level Augmentation Service (CLAS):** Tailored for users in Japan, this variant utilizes QZSS L6 signals to provide free PPP corrections without external services. It is ideal for land and marine navigation in Japan.

All GNSS variants integrate seamlessly with SBG Systems' antenna portfolio and Qinertia post-processing software. *www.sbg-systems.com*

EOLTS: Revolutionizing End-of-Life Tracking for Spacecraft

As space becomes increasingly crowded, managing decommissioned satellites is critical for sustainable operations. Syntony, with the support of CNES, is developing the End-Of-Life Tracker for Spacecraft (EOLTS) tracker—an innovative, low-power GNSS-based solution that provides precise and autonomous tracking of space systems at the end of their operational life. This breakthrough technology enhances Space Situational Awareness (SSA) and supports sustainable space initiatives.

With thousands of active and defunct satellites orbiting Earth, space debris poses an escalating threat to operational space missions. Uncontrolled satellites can collide, creating hazardous debris fields that jeopardize space infrastructure. To address this, CNES initiated the "T4SC" (Tech for Space Care) program, aimed at developing advanced technologies to tackle the different issues of space debris.

NovAtel partnership with GPR, Inc.

NovAtel will enhance its industry-leading SPAN GNSS+INS (Global Navigation Satellite Systems + Inertial Navigation System) solution by adding ground-penetrating radar sensors. It signed a MoU with Massachusetts-based GPR, Inc. to integrate GPR's WaveSense ground-penetrating radar technology.

NovAtel will explore the full potential of integrating its renowned SPAN system with GPR's unique subsurface mapping technology. This exploration aims to deliver customers a robust positioning solution, ensuring consistent, centimetre-level accuracy even in GPS-denied or environmentally challenging conditions in autonomy, mining and other mission-critical applications. *novatel.com*

GMV to support evolution of GRC

The European Union Agency for the Space Programme (EUSPA) has awarded GMV a framework contract to advance the Galileo Reference Centre (GRC), a key facility for monitoring and evaluating the performance of the Galileo satellite navigation system.

The upcoming GRC V2 version will introduce real-time monitoring capabilities, enhancing EUSPA's ability to oversee GNSS services. This evolution will support additional Galileo services, including:

- **Signal Authentication Service (SAS):** Strengthening trust in Galileo signals.
- **Time Dissemination Service:** Enabling precise synchronization for critical infrastructure.
- **Search and Rescue (SAR):** Improving emergency response operations.
- **Emergency Warning Satellite Service (EWSS):** Facilitating public alerts for natural disasters and emergencies.

The upgraded GRC is expected to be operational by 2026 without impacting ongoing functions. *www.gmv.com*

GEODNET raises $8M to equip humanoid robots with cm-level accuracy

GEODNET Foundation has announced an $8M strategic round led by Multicoin Capital with participation from ParaFi and DACM, bringing the project's total financing to date to $15M. The foundation will use the capital to service the network's rapidly-growing customer pipeline and support new robotics and physical artificial intelligence (AI) applications and customers. Real-time kinematics (RTK) is a navigation technique that enhances positioning data from satellite-based systems—such as GPS, GLONASS, Galileo, or BeiDou—to achieve real-time, centimeter-level accuracy. GEODNET recently became the largest RTK network in the world and now boasts more than 13,500 user-deployed reference stations across 4,377 cities in more than 142 countries. These stations provide precision location services to thousands of robots daily, including autonomous trucks, construction vehicles, agricultural equipment, drones, robotic lawn mowers, robotic marine vehicles, and much more. *www.geodnet.com*

Zephr.xyz wins $1.7M AFRL contract

Zephr.xyz has been awarded a $1.74 million Small Business Innovation Research (SBIR) Direct-to-Phase II contract from the Air Force Research Laboratory (AFRL) to develop an advanced capability to strengthen operational awareness and resilience for U.S. warfighters. The new system will provide real-time detection of GPS/GNSS jamming and spoofing in

SUBSCRIPTION FORM

YES! I want my Coordinates

I would like to subscribe for (tick one)

☐ 1 year	☐ 2 years	☐ 3 years
12 issues	24 issues	36 issues
Rs.1800/US$140	Rs.3400/US$200	Rs.4900/US$300
*		SUPER saver

First name ....

Last name ....

Designation ....

Organization ....

Address ....

....

City .... Pincode ....

State .... Country ....

Phone ....

Fax ....

Email ....

I enclose cheque no. ....

drawn on ....

date .... towards subscription

charges for Coordinates magazine

in favour of **'Coordinates Media Pvt. Ltd.'**

Sign .... Date ....

Mail this form with payment to:

Coordinates
A 002, Mansara Apartments
C 9, Vasundhara Enclave
Delhi 110 096, India.

If you'd like an invoice before sending your payment, you may either send us this completed subscription form or send us a request for an invoice at iwant@mycoordinates.org

* Postage and handling charges extra.

MARK YOUR CALENDAR

April 2025

GISTAM 2025
1-3 April
Porto, Portugal
https://gistam.scitevents.org

Geo Connect Asia, Digital Construction Asia, Drones & Uncrewed Asia
09 - 10 April 2025
Singapore
https://connect.geoconnectasia.com/partners-coordinates

Assured PNT Summit
23-24 April 2025
Washington DC, USA
https://pnt.dsigroup.org

May 2025

17th Baška GNSS Conference
11-15 May 2025
Baška, Croatia
https://rin.org.uk

GeoIgnite
12-14 May2025
Ottawa, Canada
https://geoignite.ca

June 2025

GEO Business 2025
04-05 June
London, UK
www.geobusinessshow.com

July 2025

Esri User Conference
14-18 July 2025
San Diego, USA
www.esri.com

September 2025

Commercial UAV Expo 2025
2-4, September
Las Vegas
www.expouav.com

Esri India User Conference 2025
September - Delhi 3rd & 4th, Kolkata 9th, Hyderabad 10th, Mumbai 12th
www.esri.in

ION GNSS+
08-12 September 2025
Baltimore, USA
www.ion.org

October 2025

The Arab Conference on Astronomy and Geophysics
13 - 16 October 2025
Cairo, Egypt
https://acag-conf.org

November 2025

Canada's National Geomatics Expo 2025
3 - 5 November
Calgary, Canda
https://gogeomaticsexpo.com

contested domains while geolocating the sources of these attacks. As part of the program, Zephr.xyz's dual-use "networked GNSS" technology – which turns ordinary mobile phones into a high-fidelity GNSS receiver network – will undergo rigorous field testing in Ukraine and multiple U.S. military exercises before integration with the Department of Defense's Tactical Assault Kit (TAK) and the Department of Homeland Security's Team Awareness Kit (TAK). *www.Zephr.xyz*

Production of MAPS Gen II system by Collins Aerospace

Collins Aerospace has received approval for Full Rate Production of the Mounted Assured Positioning, Navigation and Timing (PNT) Generation II system (MAPS GEN II). Following the fifth delivery order of the jam-and-spoof-resistant navigation solution, Collins will produce thousands of MAPS units for installation on U.S. Army and U.S. Marines Corps' combat ground vehicles including military watercraft. MAPS fuses sensor data including satellite navigation information and secured positioning, navigation and timing data for crewed and uncrewed ground vehicles. MAPS GEN II is comprised of the company's NavHub™-100 navigation system and Multi-Sensor Antenna System (MSAS-100) and supports multiple mission sets including combat, artillery fires, air and missile defense, ship-to-shore and contested logistics. *rtx.com*

SparkFun Electronics unveils surveying receiver

SparkFun Electronics has released the SparkPNT RTK Facet mosaic L-Band, a high-precision geolocation and surveying receiver. It features Septentrio's multi-band mosaic-X5 and offers centimeter-grade measurements with 6 mm RTK fixes available in less than one minute, according to Sparkfun. The receiver can connect to phones or tablets via Bluetooth, allowing NMEA output compatibility with most geographic information system software. It uses u-blox's PointPerfect service for corrections, broadcast from a geosynchronous Inmarsat satellite. *www.sparkfun.com*